MASSACHUSETTS INSTITUTE OF TECHNOLOGY

104p

TE-11

TOWARDS A LOW LEVEL ACCELEROMETER

by

Shaoul Ezekiel

June 1964

Degree of Master of Science

EXPERIMENTAL ASTRONOMY LABORATORY
MASSACHUSETTS INSTITUTE OF TECHNOLOGY
CAMBRIDGE 39, MASSACHUSETTS

TOWARDS A LOW LEVEL ACCELEROMETER

by

SHAOUL EZEKIEL
B.Sc., Imperial College of
Science and Technology
(1957)

SUBMITTED IN PARTIAL FULFILLMENT
OF THE REQUIREMENTS FOR THE
DEGREE OF MASTER OF SCIENCE

at the
MASSACHUSETTS INSTITUTE OF TECHNOLOGY
June, 1964

Signature of Author _____
Department of Aeronautics and
Astronautics, June 1964

Certified by _____
Thesis Supervisor

Certified by _____
Thesis Supervisor

Accepted by _____
Chairman, Departmental
Graduate Committee

TOWARDS A LOW LEVEL ACCELEROMETER

by

Shaoul Ezekiel

Submitted to the Department of Aeronautics and Astronautics on May 22, 1964 in partial fulfillment of the requirements for the degree of Master of Science.

ABSTRACT

A preliminary investigation is made into a low level accelerometer incorporating a diamagnetically supported magnet inside a superconducting tube. Low level control forces are examined and the magnetic force is found most suitable. Light pressure exerts a measureable force and is suggested for calibration.

The feasibility of closing a feedback loop around the magnet is demonstrated. The accelerometer shows much promise for application below 10^{-6}g and the performance results obtained so far are limited only by displacement detector sensitivity and noisy environment.

Thesis Supervisor: Yao T. Li
Title: Professor of Aeronautics and Astronautics

Thesis Supervisor: John G. King
Title: Associate Professor of Physics

ACKNOWLEDGEMENTS

The author wishes to express his appreciation to the following persons: Professor Yao T. Li and Professor John G. King for their encouragement and council, Philip K. Chapman for his interest and valued cooperation, throughout the project, Professor Winston Markey, J. T. Egan, D. R. Jankins, C. L. Lothrup, W. Littlewood and Mrs. Hunt of the Experimental Astronomy Laboratory for their able assistance in all phases, Professor Samuel Collins and Robert Cavileer of the Cryogenic Laboratory for their efforts in providing liquid helium and other cryogenic equipment, and Miss Pat Beliveau for typing the manuscript.

This research was carried out under DSR Contract 5007, sponsored by NASA, under Grant Number /NsG 254-62./

TABLE OF CONTENTS

Figures

CHAPTER 1

INTRODUCTION

The need for low level acceleration or force measuring devices is rapidly increasing. As inertial instruments become more sensitive, their testing becomes more elaborate. Vibration isolation and seismic noise filters help to provide a relatively stable test base.

Continuous low thrust space vehicles require accelerometers with sensitivities below 10^{-5}g. The calibration and test of such accelerometers on earth is not elementary.

An investigation into the design of a low level single axis accelerometer in the micro-g sub-micro-g level is being presently conducted at the Experimental Astronomy Laboratory of the Massachusetts Institute of Technology.

In LLAMA, acronym for Low Level Acceleration Measurement Apparatus, it is proposed to use a magnet which is diamagnetically supported inside a superconducting tube as the proof mass, a displacement detector sensitive to the slightest axial motion of the magnet, a low level restoring force to bring the magnet back to null and a means for low-g calibration.

This thesis is concerned in examining possible sources of low level force in the 10^{-3}-10^{-6} dynes range for the control of the magnet and in investigating, in a preliminary fashion, the feasibility of a low level accelerometer incorporating this method of suspension.

CHAPTER 2

THE SUSPENSION

2.1 Ideal Suspension

The ideal suspension for this application is one that, along one axis there exists a zero force or neutral region that exhibits no stiction, friction, or hysteresis so that the application of the smallest force will cause the supported member to displace from its rest position.

2.2 Diamagnetic Suspension

The diamagnetic or Meissner effect suspension is the subject of a Masters Thesis by P.K. Chapman[1]. A brief description is given here.

When a metal such as lead or niobium is cooled, its resistance drops with decrease in temperature until a critical temperature is reached ($7.1^{o}K$ for lead and $8^{o}K$ for niobium) when suddenly the material loses all its resistance and becomes what is termed, a superconductor.

A superconductor displays the property of expelling all magnetic fields within it, i.e., it becomes perfectly diamagnetic. This latter property is termed the Meissner Effect.[2,3]

If a small magnet is lowered over a superconducting plane, the flux of the magnet cannot penetrate the superconductor and will be squashed, see Figure 2.2-1, thus resulting in an upward force. If the mass of the magnet is chosen correctly, relative to its pole strength and dimensions, this upward force can be sufficient for supporting the magnet.

If the magnet moves horizontally, this support force moves along also, so that the suspension is stable in the vertical direction.

In LLAMA, the magnet is floated at the center of a superconducting tube so that it is free along the polar axis of the tube and in stable equilibrium along the other two axes.

2.3 Suspension Characteristics

Experiments showed that the magnet tended to be expelled from the tube. According to the model developed in Ref. 1, the force acting on the magnet when displaced from the center of the tube is

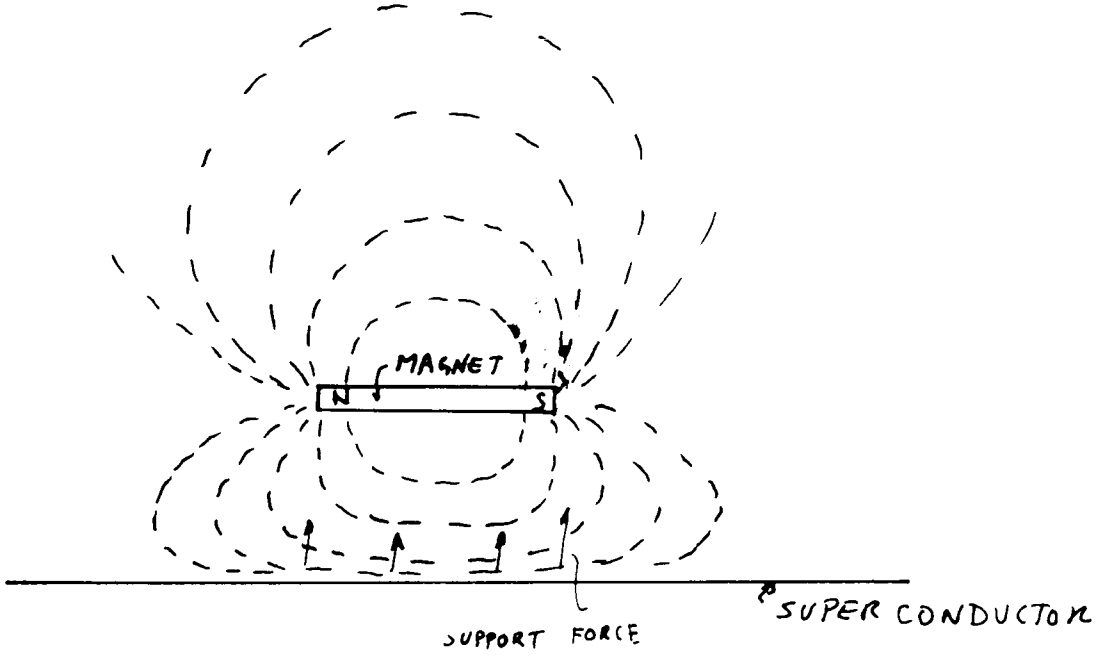

FIG 2·2—1 MAGNET SUPPORTED OVER A SUPER CONDUCTOR

$$F_x = -\alpha \sinh 2 c x$$

where

F_x = force on magnet at axial displacement x from null

α = constant -- depends on geometry of tube and the magnet and the pole strength of the magnet

c = constant -- depends on the radius of the tube

A sketch of the variation of the force with displacement is shown in Figure 2.3-1. Although the suspension is unstable in the axial direction, that is any displacement of the magnet from null will cause it to be expelled, the initial negative spring constant is claimed to be very small. More important is that the suspension exhibits no stiction -- a property so vital for the detection of small forces.

2.4 The Suspended Element

The suspended element is an Alnico V magnet 1.6 cm long, 0.3 cm in diameter, and weighing 1 gram.

The float height was 1.5 mm below the centre of the 25 mm diameter superconducting tube. A photograph of the

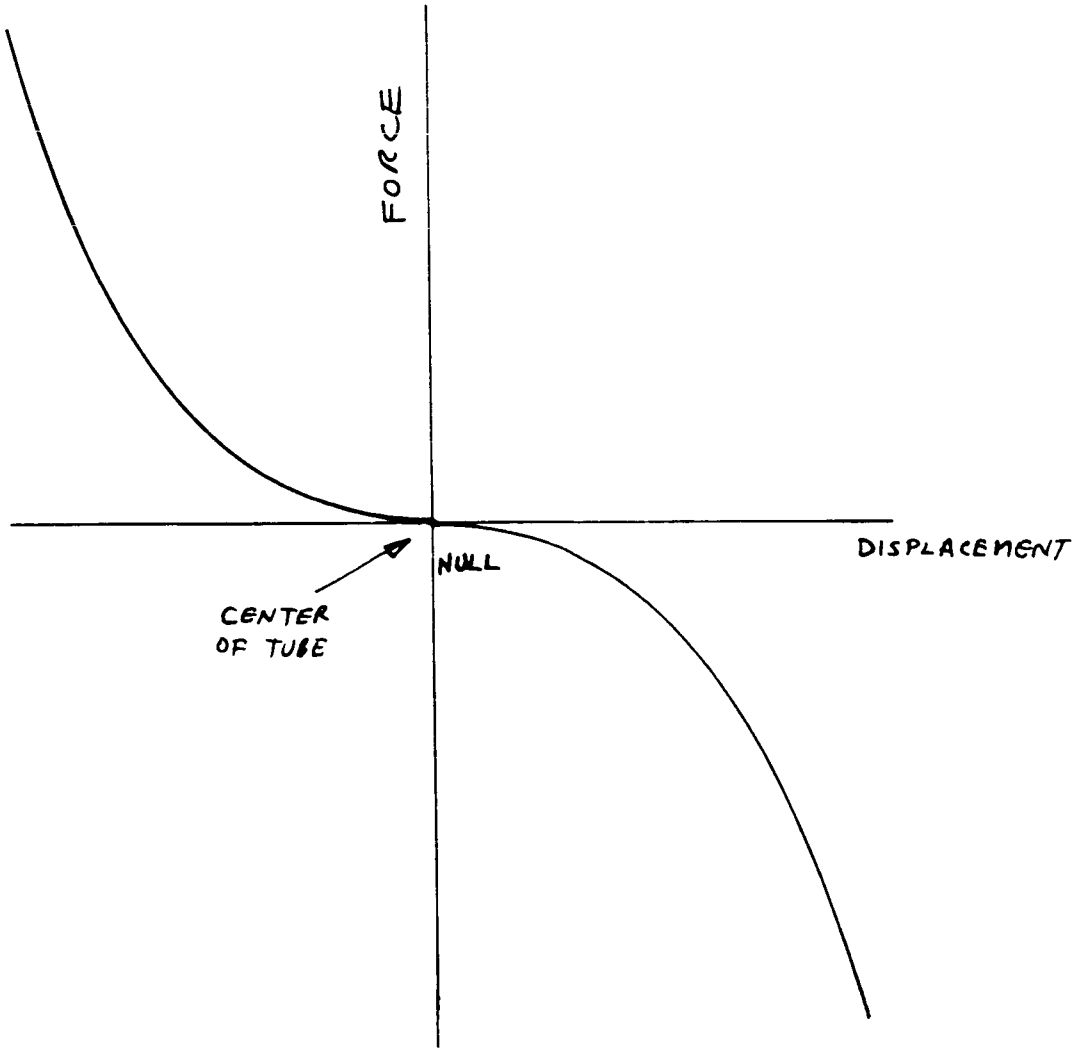

FIG 2.3-1 SUSPENSION FORCE INSIDE A SUPER CONDUCTING TUBE

floating magnet is shown in Figure 2.4-1. The magnet has a 1 cm diameter aluminum disc at each end.

2.5 The Dewar

The basic construction of the metal dewar is shown in Figure 2.5-1, and the details are given in Ref. 1.

Niobium (or columbium) sheet is wrapped around a copper tube housed in a copper block which is attached to the bottom of a liquid helium inner bottle . A vacuum outer jacket surrounds this bottle.

Two windows in the outer jacket enable the magnet to be viewed from both ends. The magnet is stored in an "ante chamber" while the niobium is cooled to avoid flux trapping and is inserted into the tube by means of a spoon manipulated from outside via 'o' ring feed through.

The base of the dewar rests on a 3 point support so that by varying the length of one of the supports, small tilt angles can be applied.

2.6 Suspension Damping

Some degree of eddy current damping is provided by the presence of the copper tube inside the superconducting tube. Experiments have indicated a damping time constant of 3 seconds.

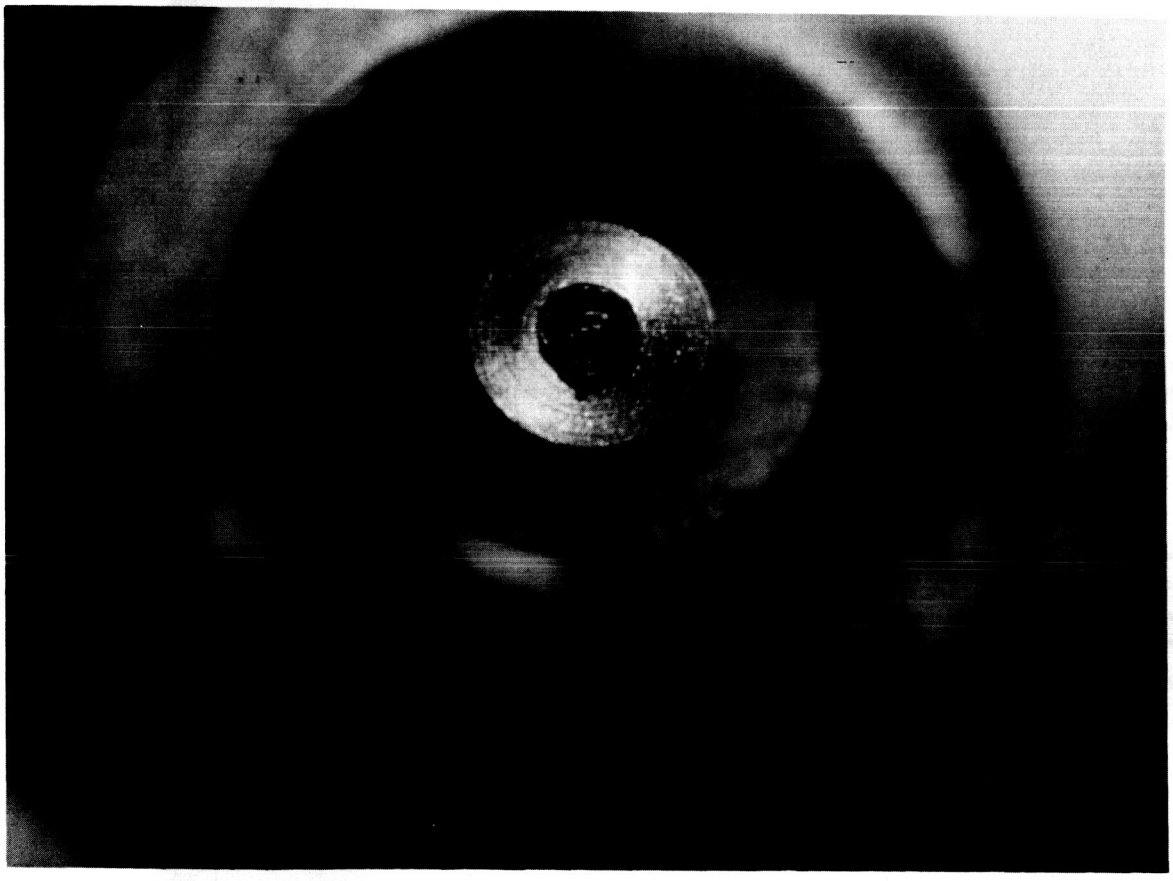

Figure 2.4-1 Magnet Floating Inside Superconducting Tube

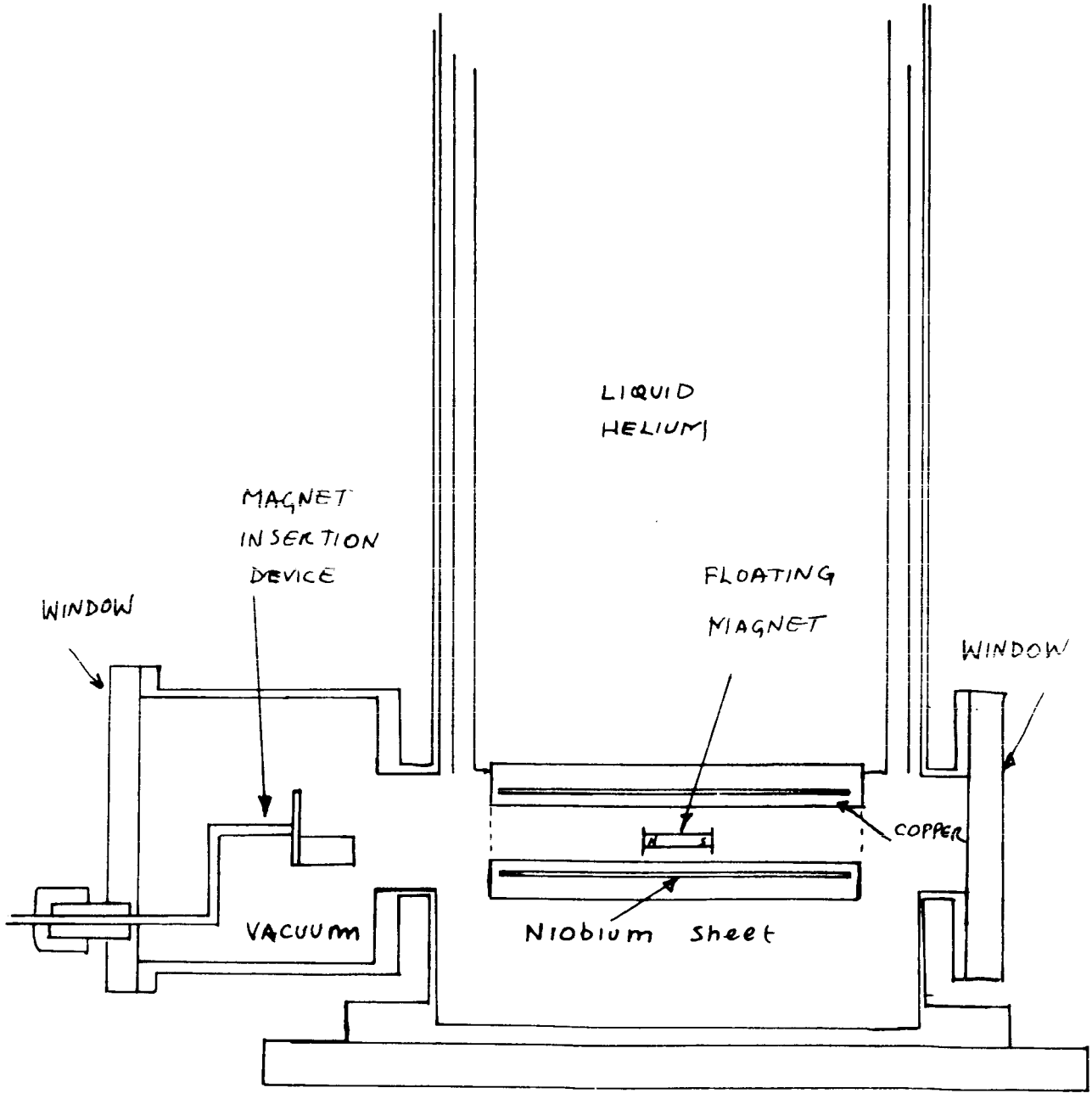

FIG 2·5—1 BASIC CONSTRUCTION OF METAL DEWAR

CHAPTER 3

LOW LEVEL FORCES

3.1 Need for Low Level Forces

If LLAMA is subjected to an acceleration of 10^{-6}g along its sensitive axis, a restoring force of about 10^{-3} dynes would be needed to keep the 1 gram magnet at its null position. Increasing the range below a micro-g means the need for even smaller forces.

Possible sources of such low force are examined in this Chapter and the applicability to LLAMA, if any, is discussed.

3.2 Ideal Low Level Force

The ideal force for LLAMA is the one that

(a) has adequate range, 10-^{3} - 10^{-6} dynes

(b) is simple to generate

(c) is simple to control -- preferably with non-mechanical means

(d) its magnitude is readily measurable, since below 10^{-3} dynes, no suitable means exist for

calibration

(e) is compatible with the LLAMA system.

It is desirable to have the range extend up to 10^{-3} dynes and above so that the method of measurement of the force can be checked against available methods.

3.3 Beam Forces

Forces that involve the change of momentum of particles are termed, here, beam forces. Since the aim is for low level forces, particles of small mass are considered, beginning with the "zero" mass photon.

3.3.1 Photon Force

Light has been assumed to exert pressure ever since Kepler (1619).[4] Lebedev and Hull (1903) managed to separate light pressure from thermal effects or radiometer effect by conducting their experiments at very low atmospheric pressure.[5]

The corpuscular theory of light pressure is presented in Appendix A. The theory indicates the force F_{ph} of light or, better, electromagnetic radiation to be

$$F_{ph} = \frac{E\,A\,(1 + r)\,\cos^2\theta \times 10^7}{c} \qquad (3.3.1\text{-}1)$$

where

F_{ph} = force exerted by beam of light in dynes

E = power in incident beam in watts

c = velocity of light = 3×10^{10} cm/sec

r = reflectivity of surface on which the beam is incident

θ = the angle of incidence of beam on the surface

A = area of surface in cm^2

The magnitude of this force is 0.66×10^{-3} dynes if the energy in the beam is 1 watt falling normally on a perfectly reflecting surface.

The force exerted by light or electromagnetic radiation will be referred to, from here on, as photon force.

The photon force can be estimated according to equation (3.3.1-1) by measuring the power in the beam, plus a knowledge of the reflectivity of the surface for the wavelength of the radiation, the area of the surface and the angle of incidence. n other words, an estimate of the force can be made externally without the need for calibration.

For LLAMA application, the available surface area can be increased by attaching an aluminized disc to either end of the magnet. Because of the float height, the limit on the size of the disc in the present set up is about 1 sq. cm. In order to exert 10^{-3} dynes, a beam power density of 1.5 watts/cm^2 is needed. To generate this power density may be practical but to go much higher is not possible with present sources.

The main requirement for the application of a photon force is a high vacuum environment below 10^{-5} torr to avoid thermal effects (see Sec. 3.3.3).

3.3.2 Photo-Electron Force

If a beam of light or photons falls, not on a reflecting surface but instead on a photoemissive surface, electrons will be emitted. The number of electrons is proportional to the number of photons falling on the surface. However, the energy of each emitted electron depends on the wavelength of the photon and is given according to the Einstein Law

$$e(V + \phi) = \frac{hc}{\lambda}$$

where

e = the charge of an electron

ϕ = work function of surface material

h = Plank's constant

c = velocity of light

λ = wavelength of photon

V = energy of electron in volts

eV = total energy of electron in electron volts

thus

$$eV = \frac{hc}{\lambda} - e\phi$$

or

$$eV = \frac{hc}{\lambda} - \frac{hc}{\lambda_o}$$

where

λ_o = critical wavelength = $\frac{hc}{e\phi}$

but

$$eV = \frac{1}{2} m_e v_e^2$$

where

m_e = mass of electron

v_e = velocity of electron

$$\therefore \quad v_e = \sqrt{\frac{2hc}{m_e} \quad \frac{\lambda_o - \lambda}{\lambda \lambda_o}}$$

The momentum of an electron is

$$m_e v_e = \sqrt{2hc\, m_e \frac{\lambda_o - \lambda}{\lambda \lambda_o}}$$

and the momentum of a photon is

$$\frac{h\nu}{c} = \frac{h}{\lambda}$$

and the increase in momentum due to electron emission is

$$\xi = \frac{\text{momentum of emitted electron}}{\text{momentum of (responsible) incident photon}}$$

$$= \frac{\sqrt{2hc\, m_e \frac{\lambda_o - \lambda}{\lambda \lambda_o}}}{h/\lambda}$$

For example with a material such as an S_1 surface (Cesium-Silver) for which $\lambda_o = 1.2\ \mu$ and using a UV source with $\lambda = 0.4\ \mu$ and

$h = 6.6 \times 10^{-34}$ joules-sec^3

$c = 3 \times 10^8$ m/sec

$m_e = 10^{-30}$ Kg

$e = 1.6 \times 10^{-9}$ coulombs

and assuming photon and electron motion normal to surface,

$$\xi \simeq 600$$

Therefore, in this case, the effective momentum of each photon is 601 times greater than if the photon were incident on a completely absorbing surface. If the momentum of every photon is increased like this, a greatly increased force results. Unfortunately, not every photon causes an electron to be emitted. The number of electrons emitted per incident photon is Q, the quantum efficiency for the surface at the wavelength of the radiation. For the S_1 surface at $\lambda = .4\ \mu$, Q is 1.5%. For an antimony-cesium S_4 surface, Q = 16% at $\lambda = .45\ \mu$. (λ_o for this surface is .6 μ.)

In order to measure the force acting on the surface, the emitted electrons are collected by a positive plate closeby so that the current in the plate circuit is proportional to the number of electrons received, which is in turn, proportional to that part of the force contributed by the photo-emission of the electrons.

The total force is given by

$$F_{total} = F_{ph} + Qn_{ph}$$

where

F_{ph} = photon force on a perfectly absorbing surface

n_{ph} = number of photons incident on surface --
(proportional to the power in the beam)

if $Q\xi >> 1$

$$F_{total} = Qn_{ph} \qquad (3.3.2\text{-}1)$$

but Qn_{ph} = the number of electrons collected by the plate

$= n_e$

$F_{total} = n_e \xi$

is a constant if the wavelength of the incident photons remains constant.

So that by simply measuring the current in the plate circuit, the force on the surface can be determined.

The assumptions in Eq. (3.3.3-1) are that

(a) the quantum efficiency of the photo-emissive surface remains constant

(b) the direction of the photons and emitted electrons is normal to the surface or close to normal

(c) all the electrons are collected by the plate

(d) the photo-emissive surface never becomes more positive than the collector plate.

As electrons are emitted, the photo emissive surface becomes positively charged. The charge in time could exceed

that on the collector plate and no more electrons would be collected -- hence the need for flushing the photo emissive surface with electrons every so often.

3.3.3 Radiometer Force[6]

Another method of exerting a force using a light beam is the radiometer effect which is associated with Crookes. Basically, the force is exerted as follows: If the light is incident on a black surface enclosed in a given low pressure gaseous bulb, the light energy is absorbed and the temperature of the surface rises. Gas molecules that now hit the surface bounce away with an increase in velocity and hence in momentum. This change in momentum is responsible for the force on the surface in the general direction of the beam -- if the other side of the surface is made reflective the force is enhanced.

Although the resulting force is much larger by several orders of magnitude than the force generated by the photons alone, the magnitude and direction of the force is difficult to predict accurately.

Another disadvantage is that there is a time constant that could be of the order of seconds associated with this method which makes it undesirable.

3.3.4 Electron Force

Instead of a beam of photons, a beam of electrons impinging on the surface may be considered. The momentum of an incident electron is determined as follows:

The velocity of an electron is given by the equation

$$eV = \frac{1}{2} m v^2 \qquad (3.3.4\text{-}1)$$

where

e = electron charge (1.6×10^{-19} coulombs)

V = accelerating voltage in volts

m_e = mass of an electron (10^{-30} Kg)

v_e = velocity of electron in meters/sec.

from (3.3.4-1) is obtained

$$v_e = \sqrt{2 \frac{e}{m} V}$$

The change in momentum of an electron after it is stopped by the surface is mv and the force generated by a normally impinging electron is given by f_e where

$$f_e = m v = m \sqrt{\frac{2e}{m}} \sqrt{V}$$

$$= \sqrt{2 e m} \sqrt{V}$$

For n electrons per sec the force is F_e where

$$F_e = n\sqrt{2\ e\ m}\sqrt{V}$$

but $n = \frac{I}{e}$ where I is the current in the electron beam.

Therefore it can be shown that

$$F_e = \sqrt{2\ \frac{m}{e}}\sqrt{V}\quad I$$

or

$$F_e = 3.5 \times 10^{-6}\quad I\ \sqrt{V}\ \text{Newtons}$$

or

$$F_e = 0.35\quad I\ \sqrt{V}\quad \text{dynes}$$

(Assuming electrons fall normally on the surface.)

For a force F_e of 10^{-3} dynes generated by using V = 400 volts requires a current of I of 0.14 mA and a power of 56 mW. These requirements are indeed feasible and can be achieved with a simple electron gun. The beam current, which is proportional to the force, if V remains constant, can be easily modulated by a voltage applied to the first grid of the gun.

This method of generating a low level force is simple, efficient and the force is easily controllable. The magnitude of the force is not limited to the **milli dyne** range and can be increased by at least two orders of magnitude.

The adaptability of this method for the application in hand is not too straightforward, as a means has to be provided for removing the incident electrons from the surface. Otherwise the surface will be charged up negatively, and a space charge will be built up around the surface. The electrons will cease to strike the surface and will be deflected away. Deflecting the electrons still constitutes a change of momentum in the direction of the beam. If this deflection is maintained at ninety degrees from the beam direction, the resulting force on the surface is the same as if the electrons were completely absorbed by the surface.

Since in the LLAMA application there is no contact with the float, removing the electrons from the surface could be done by flushing the surface with a low velocity positive ion plasma.

3.3.5 Atomic or Molecular Beam Force [7]

Still heavier particles can be used, as in an atomic or molecular beam. For the case of LLAMA, a molecular beam of Helium might be considered. The number of He molecules per second required to generate a force of 10^{-3} dynes is given by

$$F_{He} = n_{He} \times m_{He} \times v_{He}$$

or

$$n_{He} = \frac{F_{He}}{m_{He} \times v}$$

where

F_{He} = force generated by molecular beam of helium

n_{He} = number of helium molecules per second

m_{He} = mass of helium molecule

v_{He} = velocity of beam

so that for $F_{He} = 10^{-3}$ dynes and v_{He} assumed to be the velocity of sound in helium about 300 m/sec., n_{He} is 10^{16} molecules/sec.

Although LLAMA can provide the high vacuum required, the difficulty in controlling and measuring the number of molecules in the beam makes the method not too suitable.

3.4 Field Forces

Forces that can be exerted by magnetic, electrostatic and gravitational fields are examined in the following sections.

3.4.1 Magnetic Force

In air, a magnetic force can be exerted on the magnet along the sensitive axis by placing a coil on either side as shown in Figure 3.4-1. If the magnet is displaced, a small distance Δx from the midpoint between the coils, the force acting on it is

$$F = K a^2 I_1 n \left[\frac{1}{\left[a^2+(b-\ell-\Delta x)^2\right]^{3/2}} - \frac{1}{\left[a^2+(b+\ell-\Delta x)^2\right]^{3/2}} \right]$$

$$- K a^2 I_2 n \left[\frac{1}{\left[a^2+(b-\ell+\Delta x)^2\right]^{3/2}} - \frac{1}{\left[a^2+(b+\ell+\Delta x)^2\right]^{3/2}} \right]$$

where

I_1, I_2 = currents in coils 1 and 2

n = number of turns in each coil

k = constant -- depends on permeability μ_o and the pole strength of the magnet

a = mean radius of coil

2b = axial separation of coils

2ℓ = length of magnet

The force equation can be simplified by neglecting second order effects $(\Delta x)^2$ and if $I_1 = I+\Delta I$ and $I_2 = I-\Delta I$,

the following equation is obtained

$$F = k_1 nI\Delta x + k_2 n\Delta I$$

where k_1, k_2 are constants depending on b, ℓ , a and k.

The magnitude of the force, by a suitable choice of parameters, can have a wide range from less than micro dynes up to grams or more.

In LLAMA, the presence of the superconductor modifies the field inside the tube, but the general behavior of the force is retained.

Due to the complex field inside the tube, only an estimate of the force can be made externally so that some form of calibration is needed.

The force can be easily controlled by simply varying the current in the coils.

3.4.2 Electrostatic Force

The electrostatic force of attraction F between two charged plates is

$$F = 0.442 \times 10^{-6} \frac{V^2}{d^2} \quad \text{dynes/cm}^2$$

where

V = voltage across plates in volts

d = separation of plates in cm

The electric vacuum gyroscope utilizes this force for the support of the rotor.

In this case, a possible method for exerting a force on the magnet is shown in Figure 3.4.2-1.

A conducting plate, attached to each end of the magnet, is polarized by the presence of the two charged plates close to it. Attraction takes place between the magnet and the plates on one side which can be balanced by a similar force on the other side.

A net force can be exerted by varying the difference in the two voltages. Because the force level required is small, of the order of 10^{-3} dynes, the standing voltage needed can be about 100 volts and the separation around 1 cm.

For LLAMA application where there is a float height limitation, the size of the plates must be small. Also since the magnet has to be outside the tube during cooling, putting the magnet back between the two sets of plates after cooling has taken place, is a problem.

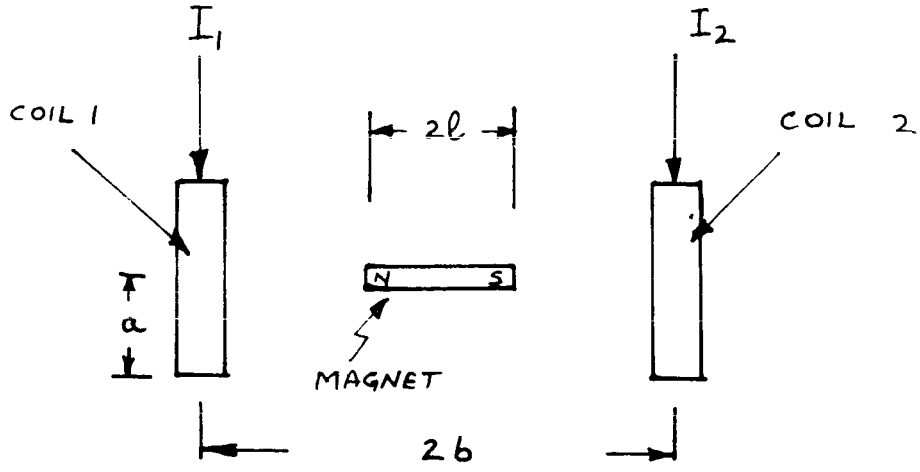

FIG. 3.4.1-1 APPLICATION OF MAGNETIC FORCE

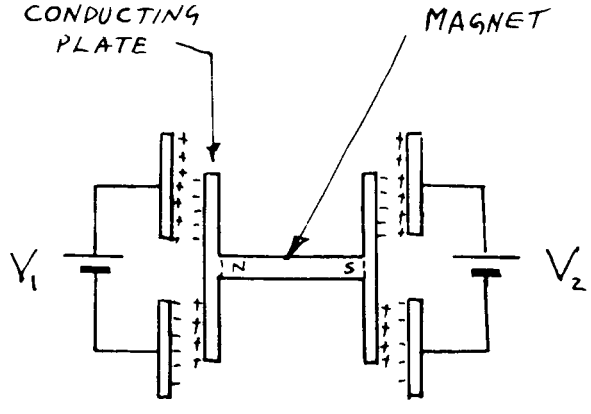

FIG 3.4.2-1 APPLICATION OF ELECTROSTATIC FORCE

3.4.3 Gravitational Force

The gravitational field of a body of known mass may be used to exert a force on the magnet. This force F_G is given by

$$F_G = \frac{GM}{r^2} \quad \text{dynes per gram (of magnet)}$$

where

G = gravitational constant = $6.7 \times 10^{-8} \frac{cm^3}{sec^2 gm}$

M = mass of body (in grams)

r = distance of body from magnet (cm)

F_G acts along the line joining the body to the magnet.

To generate 10^{-3} dynes at a distance of r = 100 cm, a mass of 1.5×10^8 gms or 147 tons would be needed, assuming M is concentrated at one point.

However, to generate 10^{-5} dynes at the same distance only requires 1.47 tons.

In order to vary the force, either the mass of the body is changed or the separation, or both. This has to be done carefully so as not to cause any vibration at the suspension. Swinging the mass along the sensitive axis generates an alternating force and has the advantage that its effect can be extracted in the presence of noise and interference by suitable filtering.

The use of the earth's gravitational field is discussed in Sections 3.5.1 and 3.5.3.

3.5 Other Methods

Forces exerted by the use of the earth's gravitational field on the earth and in space are discussed in the following sections as well as the use of the centrifugal force.

3.5.1 Table Tilt

Methods such as table tilting which use a component of the earth's gravitational field may be feasible for generating accurate forces. In the case of LLAMA, a force of 10^{-3} dynes corresponds to a table tilt of 0.2 secs. of arc, since the magnet has a mass of one gram. This small angle can be better appreciated if looked at as the angle a rigid rod 1 mile long would deflect if one end is hinged in a horizontal position and the other end depressed by $\frac{1}{20}$ inch.

To exert 10^{-6} dynes, a tilt of 0.0002 seconds of arc would be needed. The problem of generating and measuring a tilt angle of this magnitude is highly involved. A

study has been made into a possible tilting method by Blitch and Keyes.[8]

3.5.2 Centrifugal Force

(a) On Earth

The centrifugal force m RW^2 acts radially on a mass rotating with an angular velocity W at a radial distance R from the axis of rotation. Now to exert 10^{-3} dynes for the case where m = 1 gm, R = 100 cm, and angular velocity of 3.3×10^{-3} rad/sec. is required or 1.8 revolutions per hour. For a force of 10^{-6} dynes, a period of 17 hours is called for. It must be remembered that an essential requirement to avoid the g-effect is that the table must remain level to at least within .002 seconds of arc for the case of 10^{-3} dynes and .000002 seconds of arc for 10^{-6} dynes.

Clearly, the presence of the earth's field makes this method unsuitable.

(b) On a Satellite

On a satellite in a free fall orbit, the centrifugal force method could be made feasible by simply spinning the satellite at the desired angular velocity.

3.5.3 Gravity Gradient Force

Another method applicable in a satellite environment is the use of the gravity gradient. If the accelerometer or test element is lowered on a boom so that it is no longer in a free fall orbit, a net force will act on it. For example, if the length of the boom is 100 ft. and the satellite is in a near earth orbit, a force of 4×10^{-6} dynes would be exerted. Increasing this force by a substantial amount needs a much longer boom.

CHAPTER 4

RESTORING FORCE

4.1 Magnetic vs. Photon Force

From the various sources of low level force presented in Chapter 3, it is clear that the magnetic force is by far the simplest to mechanize, easy to control, gives adequate range and is very compatible with the LLAMA system. The one disadvantage is that the force needs calibration owing to the complex field inside the tube. The photon force on the other hand is capable of exerting a force that can be measured but there is a limit on its magnitude. Also, the modulation of the force becomes more complex as beam power density increases -- see Chapter 8.

For a practical system, magnetic coils will be used to provide the restoring force and the photon force will be utilized for calibration.

4.2 Magnetic Restoring Force

A magnetic restoring force may be exerted on the magnet by placing a coil coaxial with the superconducting tube on

either side of the magnet, see Figure 4.2-1.

The force due to symmetrically placed coils when the magnet is in the center of the tube is zero and builds up as either coil is approached. On the other side of each coil, the force drops to zero again.

The sum of the coil force and the suspension force, Figure 4.2-1, shows that for a given common current, the effective force in the tube can be made positive for a small region around null. Outside this region, the force decreases and eventually becomes negative. Hence a limited axially stable region results around null.

The effective force around null is desired to be as small as possible so that the magnet is free to displace under the application of the minutest acceleration.

In closed loop operation, as the magnet is displaced from null, the current in the closer coil is increased and the current in the farther coil is decreased, an increase in the effective spring constant results which drives the magnet back towards null.

Because of the superconductor[1] the force due to the coils is modified although the general behavior is retained.

For a displacement x, let $I + \Delta I$ be the current in the closer coil and $I - \Delta I$ be the current in the farther coil, the force on the magnet due to the coils is given by

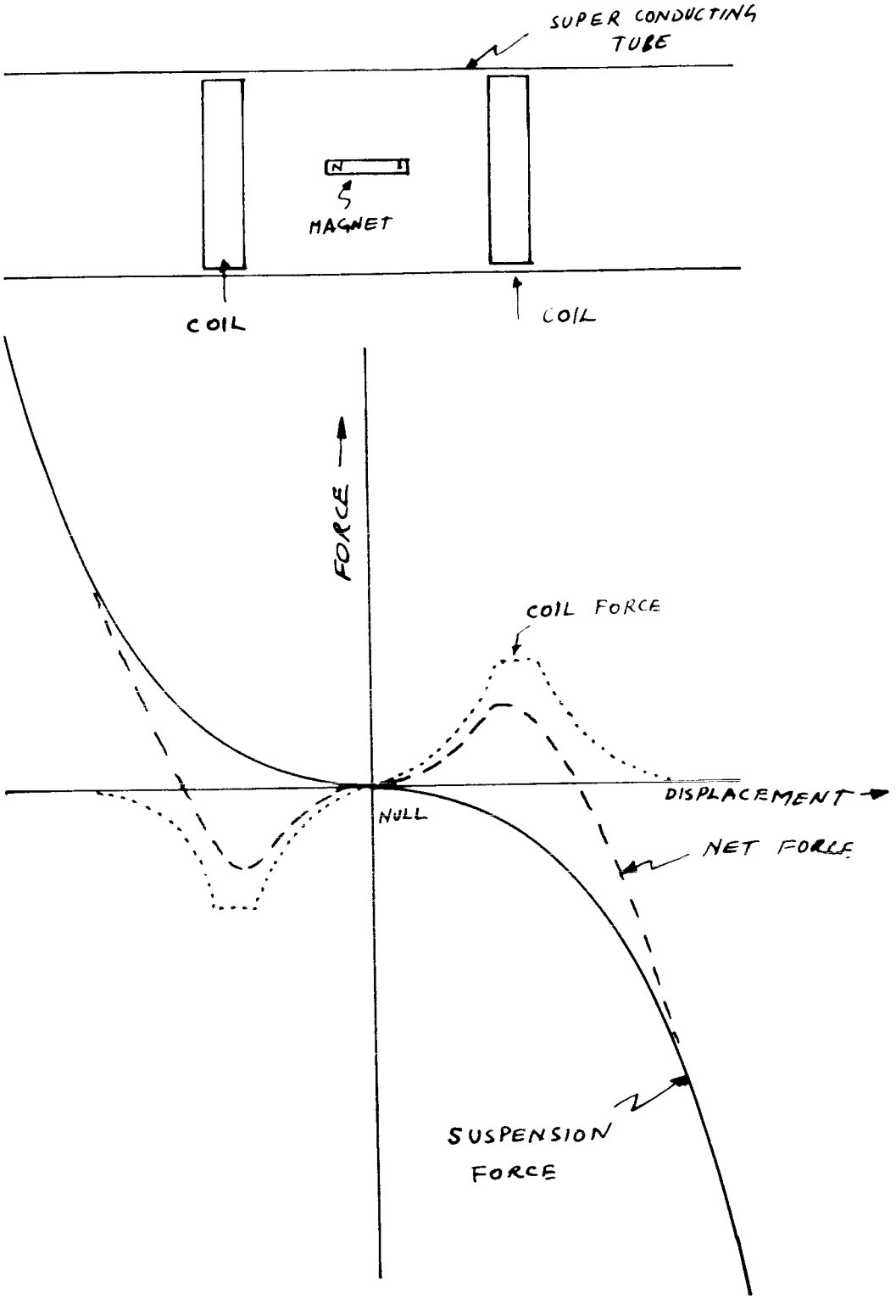

FIG. 4·2-1 FORCE ON MAGNET INSIDE TUBE

$$F_{coils} = \frac{\beta}{2} [(I+\Delta I)\, e^{cx} - (I-\Delta I)\, e^{-cx}]$$

$$= \frac{\beta}{2} I \sinh c\, x + \frac{\beta}{2} \Delta I \cosh c\, x$$

where

β = constant -- depends on the geometry of the coils and the magnet

and

c as defined in Section 2.3

If I is kept constant, ΔI can be varied at will according to the gain in the system, see Chapter 6.

That part of the magnetic force due to I, i.e., $\frac{\beta}{2} I \sinh c\, x$ is termed the common mode force because I flows in both coils. The force due to ΔI, i.e., $\frac{\beta}{2} \Delta I \cosh c\, x$ is termed the differential mode force.

The common mode force is free from dynamics since I remains constant. However, the differential mode force is associated with a lag due to the inductance of the coils.

4.3 Phase-Plane Trajectories

The equation of motion of the magnet, neglecting damping, is

$$m\ddot{x} + \frac{\beta}{2} I \sinh c x + \frac{\beta}{2} \Delta I \cosh x c - \alpha \sinh 2 c x = 0$$

where

ΔI is a function of x.

The combined effect of the suspension and magnetic forces inside the tube may then be looked at as a soft spring with the spring force eventually going negative.

The phase plane trajectories for the soft spring[9] are determined using energy methods and the general behavior is shown in Figure 4.3.1.

Near null, the closed curves represent periodic oscillations. Away from null the curves are no longer closed and the magnet is unstable.

The effect of damping is to damp out the oscillation once the magnet is inside the closed curve region.

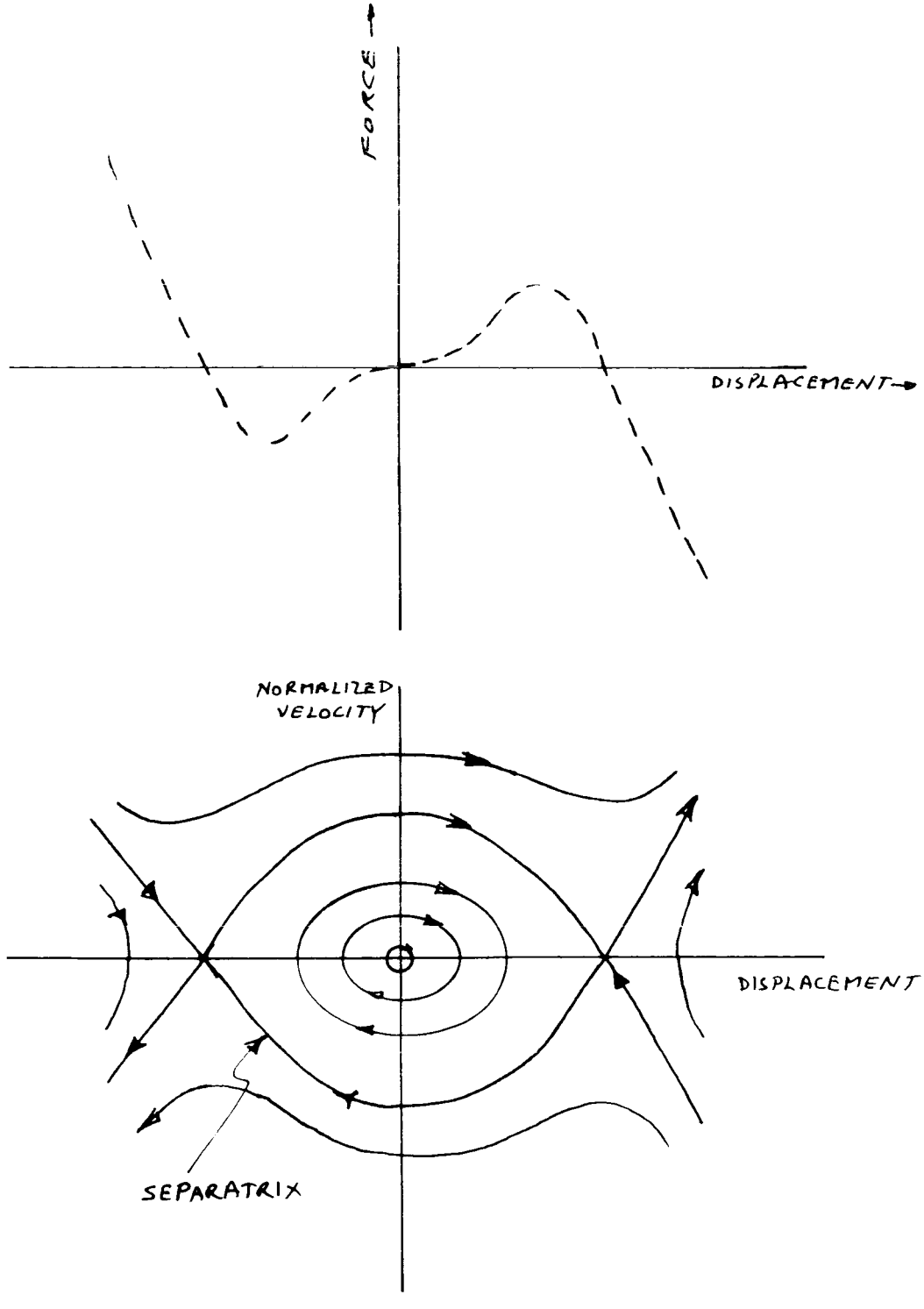

FIG. 4.3-1 PHASE PLANE TRAJECTORIES

CHAPTER 5

DISPLACEMENT DETECTION

5.1 General

If LLAMA is subjected to a low level acceleration (or g-component), the time taken for the magnet to move an appreciable distance is long. For example, if the acceleration is 10^{-6}g, the time taken to move, say 1 mm, is about 140 seconds or 0.45 secs for a displacement of 1 micron. When lower acceleration levels are considered say, 10^{-9}g, the time taken to move 1 micron is 14 seconds. Clearly, therefore, a very sensitive displacement detection is called for if a reasonable bandwidth is desired. Another reason for keeping the displacement small is to avoid the nonlinearities in the suspension and in the detector.

5.2 Ideal Detector

The ideal displacement detector for LLAMA is a device that

(a) is capable of sensing displacements way below 1 micron along the sensitive axis

(b) is insensitive to displacements along or, rotations about other axes

(c) is linear

(d) does not exert any forces on the magnet

(e) is compatible with LLAMA system.

5.3 Interferometric Method

For the LLAMA displacement detector, it is proposed to use an interferometer in the Twyman-Green configuration that utilizes, for its principal mirrors, two parallel flat mirrors mounted on either end of the magnet. This way of mounting the mirrors not only doubles the sensitivity of the normal interferometer but provides the possibility of making the instrument insensitive to motion along or about other axes.

A possible scheme that is being presently investigated, see Ref. 10 , is shown in Figure 5.3-1. One reversion prism makes the instrument insensitive to rotation of the magnet about the vertical axis and the other prism for rotation about the horizontal axis normal to the tube. Rotation about the polar axis assuming flat parallel mirror does not constitute an error.

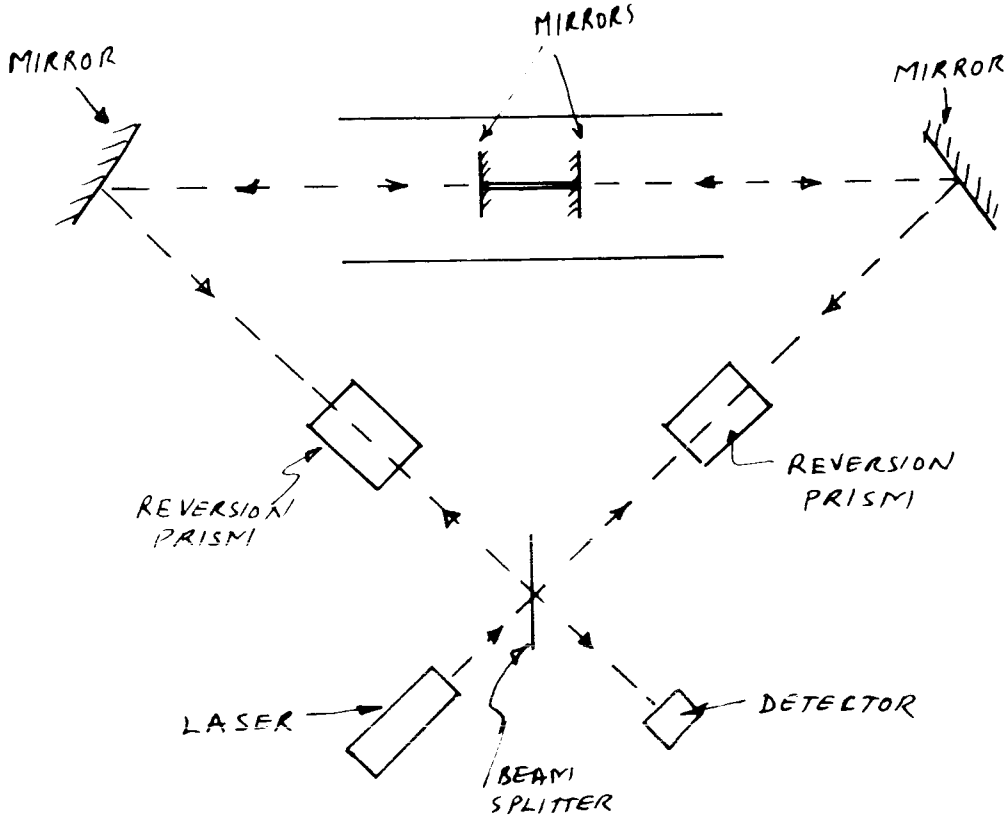

FIG. 5.3—1 INTERFEROMETER DISPLACEMENT DETECTOR

If the light from the source is highly monochromatic, coherent, and paraxial, such as that from a gas laser, the separation between fringes becomes large so that the output of the interferometer is a uniform field whose intensity is modulated by the axial motion of the magnet.

5.4 Spot Masking Method

In the absence of an interferometer, another less sensitive method for displacement detection was devised so as to carry out preliminary investigations into the suspension, the effect of the coils and the closed loop behavior.

5.4.1 Basic Configuration

The basic configuration of the system is shown in Figure 5.4.1-1.The light from a "point" source is brought to a focus at a point close to the axis of and about halfway inside the super-conducting tube via mirrors and a double convex lens. In the absence of any obstruction of the spot, the beam returns again via mirrors and a 50-50 beam splitter to a lens which brings it to a focus on a photo sensitive detector. If there is any obstruction of the spot, the output of the detector is decreased.

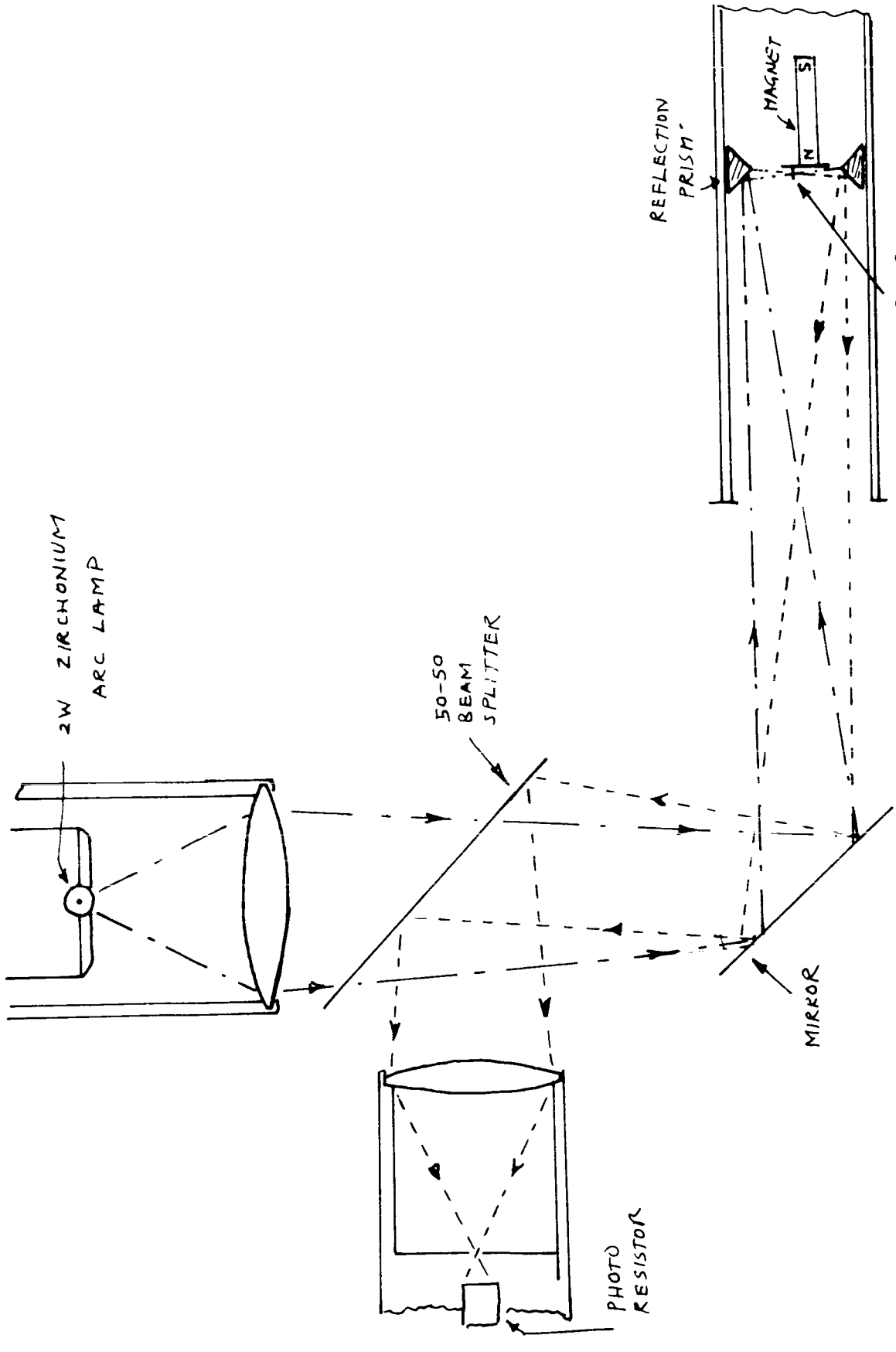

FIG 5.4-1 SPOT MASKING DISPLACEMENT DETECTOR

The spot position is chosen so that one end of the magnet when at null, masks half the spot so that motion to the left would be indicated by a decrease in output signal and similarly, motion to the right would be indicated by an increase in the output of the detector.

In order to make the range of the detector as narrow as possible, the spot size must be as small as possible, hence the need for a point source. Also, a sharp edge attached to the end of the magnet improves the linearity of the detector. A field stop at the detector helps to ensure that only the returning beam is permitted to go through to the detector.

The position of the reflecting prisms mounted inside the tube is adjusted so that the beam is normal to the axis of the tube when going from the lower prism to the upper so as to minimize the range of the detector.

A photograph of the dewar and the displacement detector is shown in Figure 5.4.1-2.

5.4.2 Design Details

The light source was a 2W Zirchonium arc lamp with a source diameter of 0.085 mm. The spot diameter was about 0.40 mm. The photo detector used was a Cadmium sulphide photo resistor and the variation of resistance with displacement is shown in Figure 5.4.2-1. This curve shows

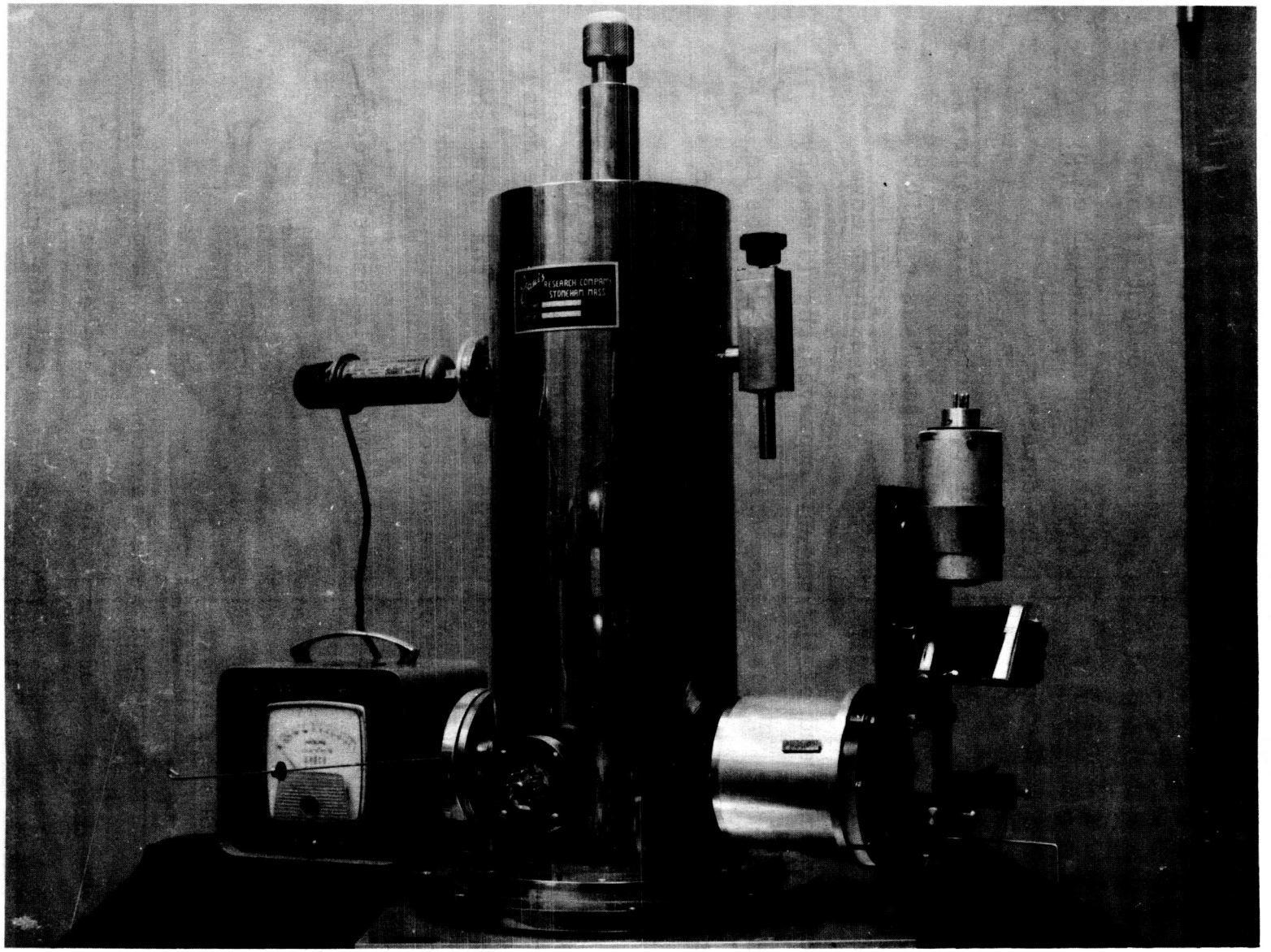

Figure 5.4.1-2 Dewar and Displacement Detector

that the resistance changes much more rapidly at low illuminations than at high ones -- a property that proves advantageous as will be shown later.

The photo resistance is incorporated in a simple bridge network shown in Figure 5.4.2-2, so that the output of the circuit is zero when the magnet is at null and is positive or negative; d.c. voltage when the magnet moves away from null. The output voltage V_o is given by

$$V_o = \frac{R_o - m R_x}{(1+m)(R_o+R_x)} V_B \qquad (5.4.2\text{-}1)$$

Eq. (5.4.2-1) indicates that if R_x is varied linearly, V_o would change more rapidly when R_x was decreasing than when increasing. The nonlinear variation in resistance shown in Figure 5.4.2-2 comes to the rescue and the resulting output curve is shown in Figure 5.4.2-3. The output curve exhibits a linear range of about 1.1 mm.

The detector has an inherent time constant which depends on the level of illumination, the higher the level the smaller the time constant. In this case, the time constant was about 0.1 seconds. The overall detection system may be then represented by the transfer function shown in Figure 5.4.2-4. A photo diode will be used in future experiments, since it has a smaller time constant.

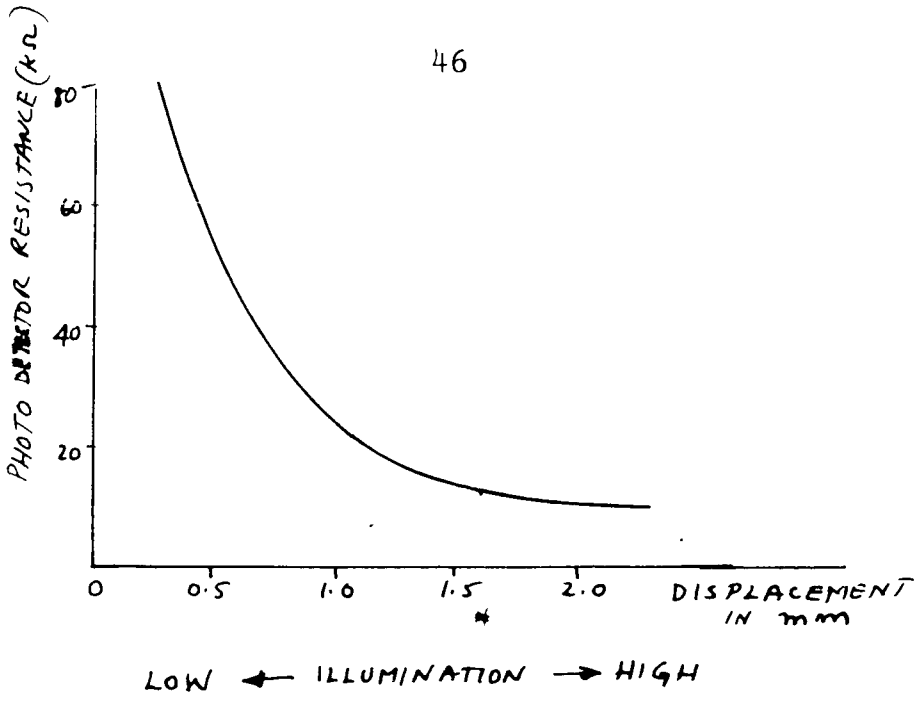

FIG 5.4.2—1 RESISTANCE OF PHOTO DETECTOR AGAINST DISPLACEMENT

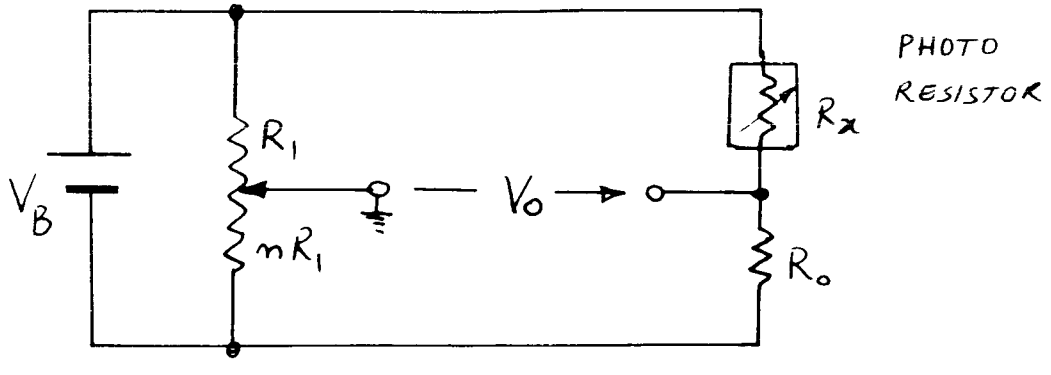

FIG. 5.4.2-2 BRIDGE CIRCUIT FOR PHOTO RESISTOR

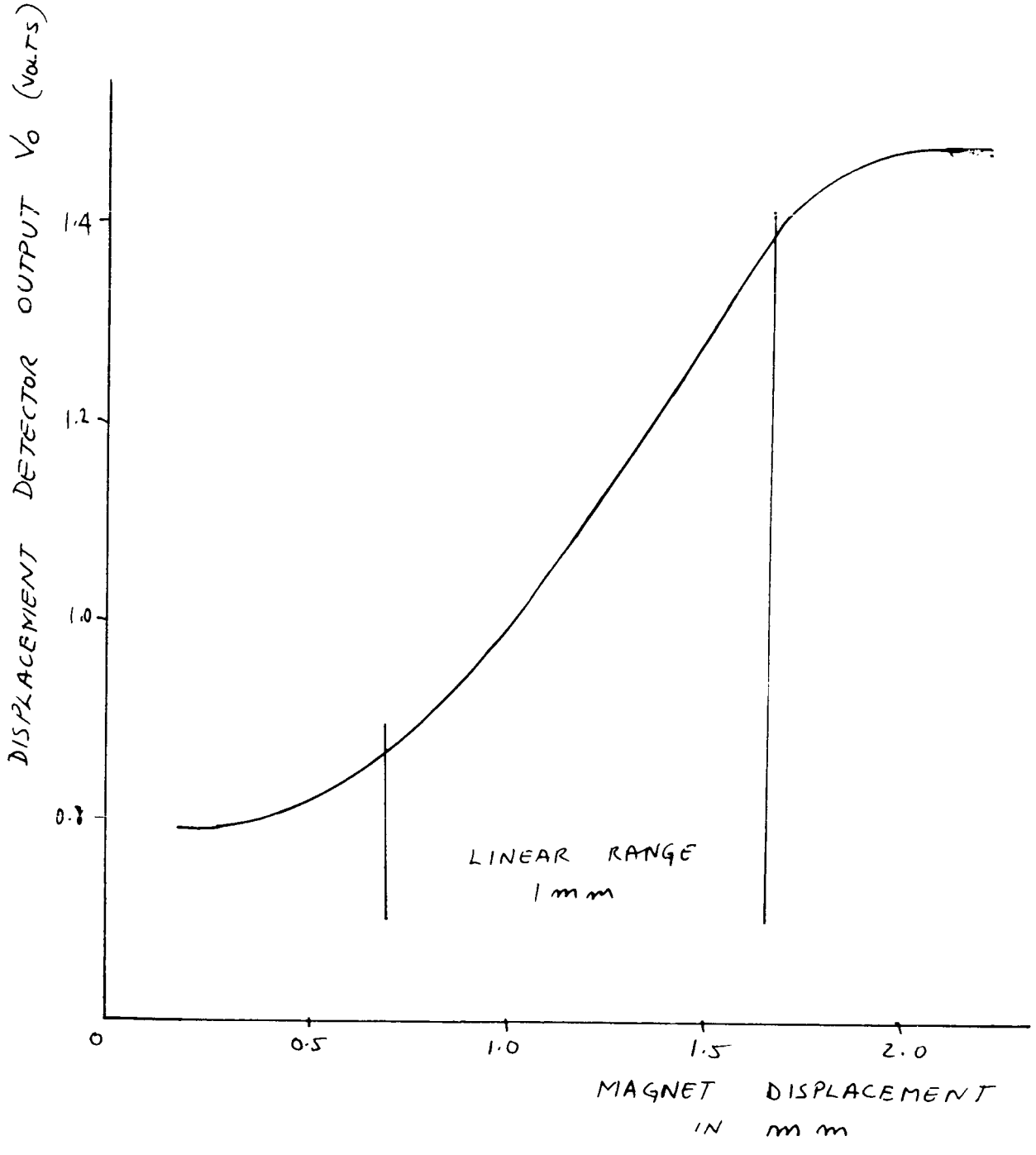

FIG 5.4.2-3 DISPLACEMENT DETECTOR SENSITIVITY

5.4.3 Lamp Output Variation

The undesirable effect of the variation in lamp output may be reduced somewhat by using another similar photo resistance in the other leg of the bridge, Figure 5.4.3-1. This compensating detector can be located on the other side of the beam splitter from the original detector so that it receives flux from the forward beam only. The flux is attenuated by a neutral density filter so that the value of the resistance of the two photo resistors is identical when the magnet is at null.

Without any variation in intensity, the output voltage V_0 is given by

$$V_o = \frac{R_o (R_x - R_{xo})}{(R_x + R_o)(R_o + R_{xo})} V_B$$

$$= \frac{(R_x - R_{xo})}{2(R_x + R_o)} V_B$$

If a change in intensity causes a change ΔR_x in R_x and ΔR_{xo} in R_{xo}, the output voltage is

$$V_0 \approx \frac{[R_x - R_{xo} + (\Delta R_x - \Delta R_{xo})]}{2(R_x + R_o)}$$

The compensation is best when $R_x = R_{xo}$, that is at null.

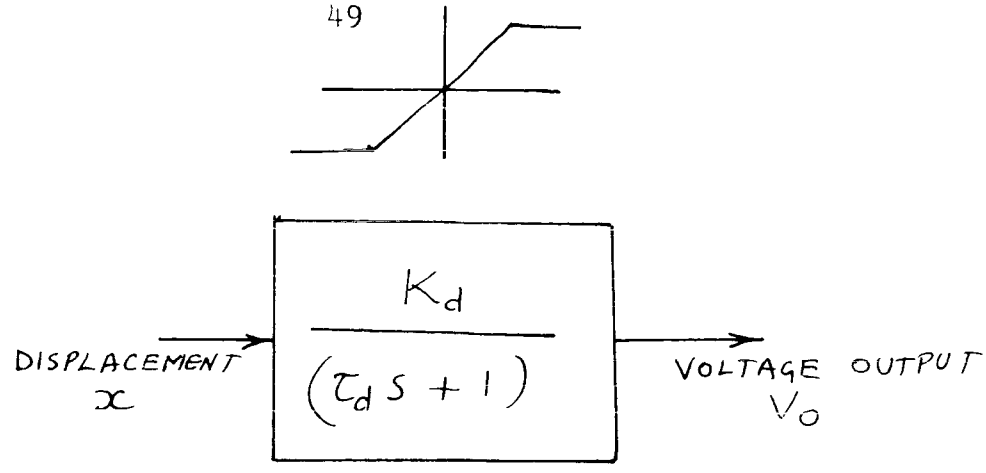

K_d = GAIN OF DISPLACEMENT DETECTOR

τ_d = TIME CONSTANT OF DISPL. DETECTOR
= 0.1 SECONDS

FIG 5.4.2-4 TRANSFER FUNCTION OF DISPLACEMENT DETECTOR

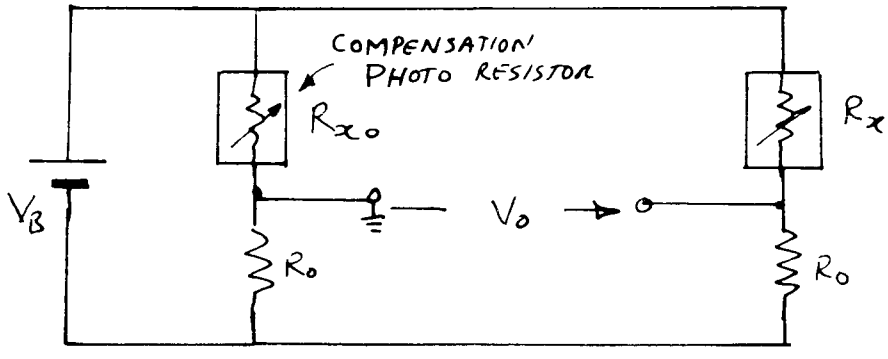

R_{xo} = VALUE OF R_x WHEN MAGNET IS AT NULL
= NORMAL VALUE OF COMPENSATION PHOTO RESISTOR

FIG 5.4.3 COMPENSATION FOR LAMP OUTPUT VARIATION

5.4.4 Sensitivity to Rotation

The present detector is sensitive to rotation of the magnet about the vertical and the transverse horizontal axes. To make it insensitive to these rotations, spherical end pieces can be attached to the magnet as shown in Figure 5.4.4-1 with the center of gravity of the magnet coinciding with the center of the sphere.

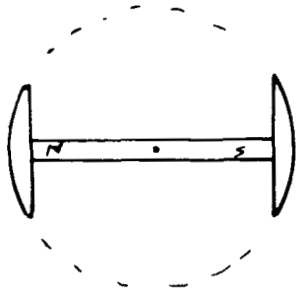

FIG 5.4.4 – 1 MAGNET WITH SPHERICAL END PIECES

CHAPTER 6

PRELIMINARY ACCELEROMETER ANALYSIS

6.1 Block Diagram

Using the information developed in preceding chapters for the various components that make up the accelerometer, an overall block diagram for the accelerometer is presented in Figure 6.1-1.

An input acceleration, a, acts on the mass of the magnet, m, to produce a force, ma. This force causes the magnet to displace from null which calls into play suspension forces, and common mode magnetic force due to a constant standing current, I. The displacement is sensed by the displacement detector which puts out an output voltage. After amplification, this voltage generates a differential mode magnetic force due to a differential current ΔI, in the coils. This force tends to drive the magnet back to null.

The suspension damping, common mode, and differential mode forces are all summed at one junction together with ma and a tilt component $mg\theta$ due to a tilt angle θ of

K_F = SUSPENSION DAMPING COEFFICIENT

K_C = GAIN OF COILS

K_a = GAIN OF AMPLIFIER

τ_c = TIME CONSTANT OF DIFF. MODE FORCE

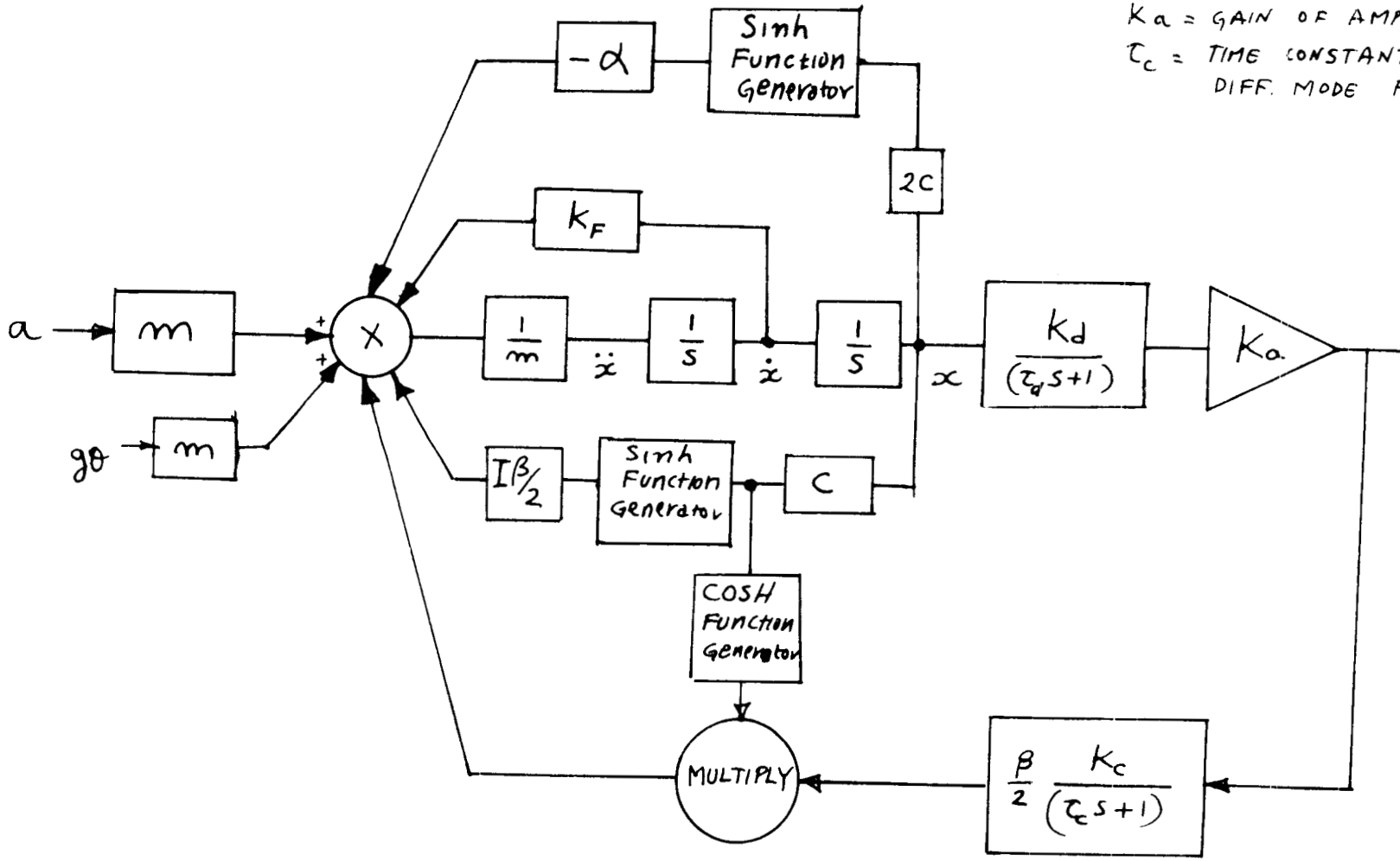

FIG 6.1-1 OVERALL BLOCK DIAGRAM FOR ACCELEROMETER

the superconducting tube.

This model of the accelerometer has many nonlinear elements -- including the fact that the displacement detector has a finite range.

6.2 Linearized Model

Since, for closed loop behavior, only small displacements are dealt with, the accelerometer model may be linearized as shown in Figure 6.2-1. This can be simplified further by absorbing the minor feedback loops as shown in Figure 6.2-2.

The open loop transfer function for the linear model is

$$\frac{\frac{\beta}{2} K_a K_d K_c \frac{1}{m}}{\left[s\left(s+\frac{K_f}{m}\right)+\frac{1}{m}\left(\frac{\beta c}{2}-2\alpha c\right)\right](\tau_a s+1)(\tau_c s+1)}$$

With the absence of damping K_f and suspension and common mode magnetic forces, the transfer function would be that of a type-2 servo, which is inherently unstable as shown in the root locus sketch in Figure 6.2-3a. Including K_f and the other forces neglected above, the root locus diagram is modified to that in Figure 6.2-3b, which is stable only for very low gain. Clearly then, some form of compensation is needed. If a pure lead compensation

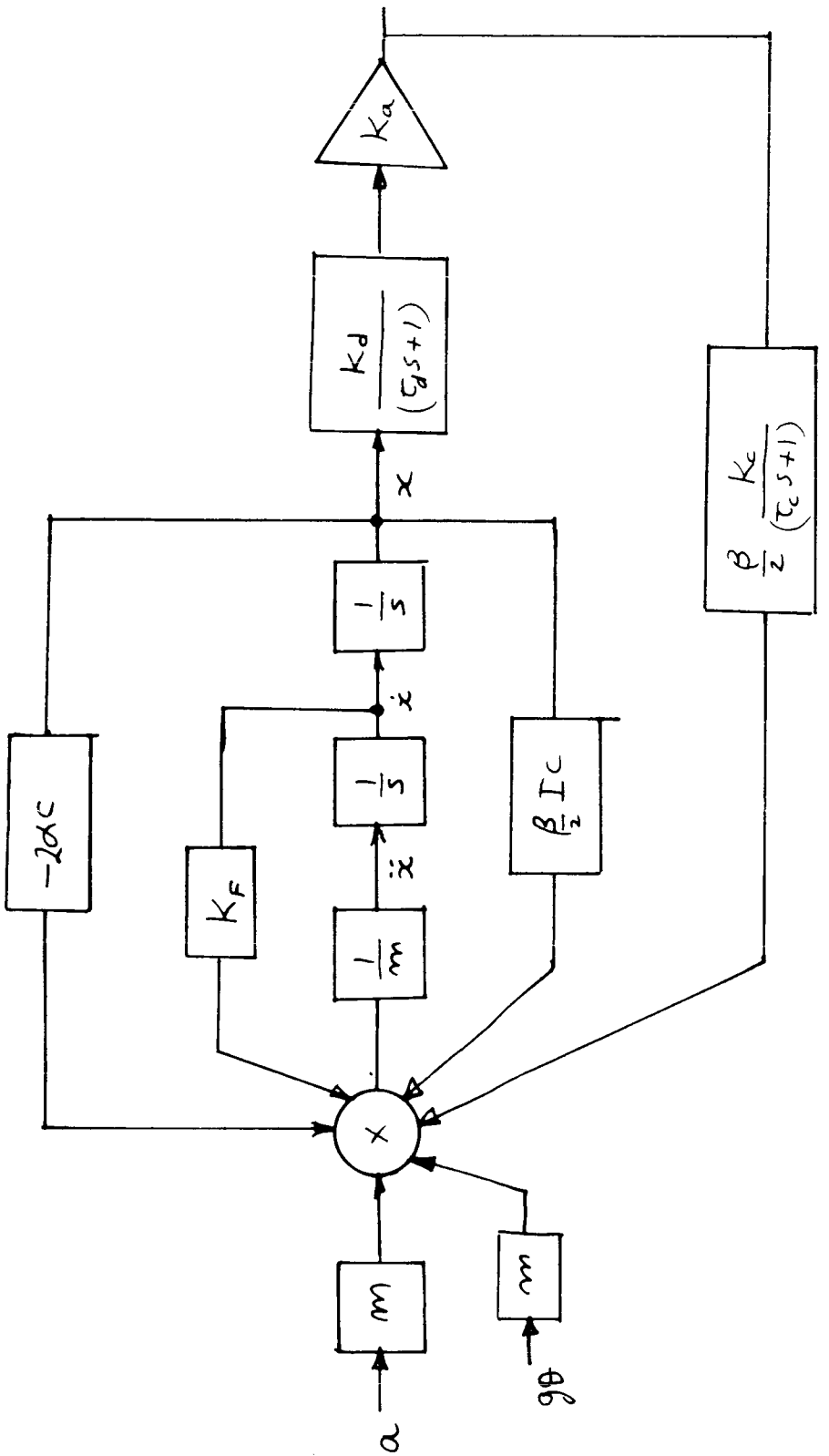

FIG 6.2-1 LINEARIZED MODEL OF ACCELEROMETER

x ASSUMED SMALL

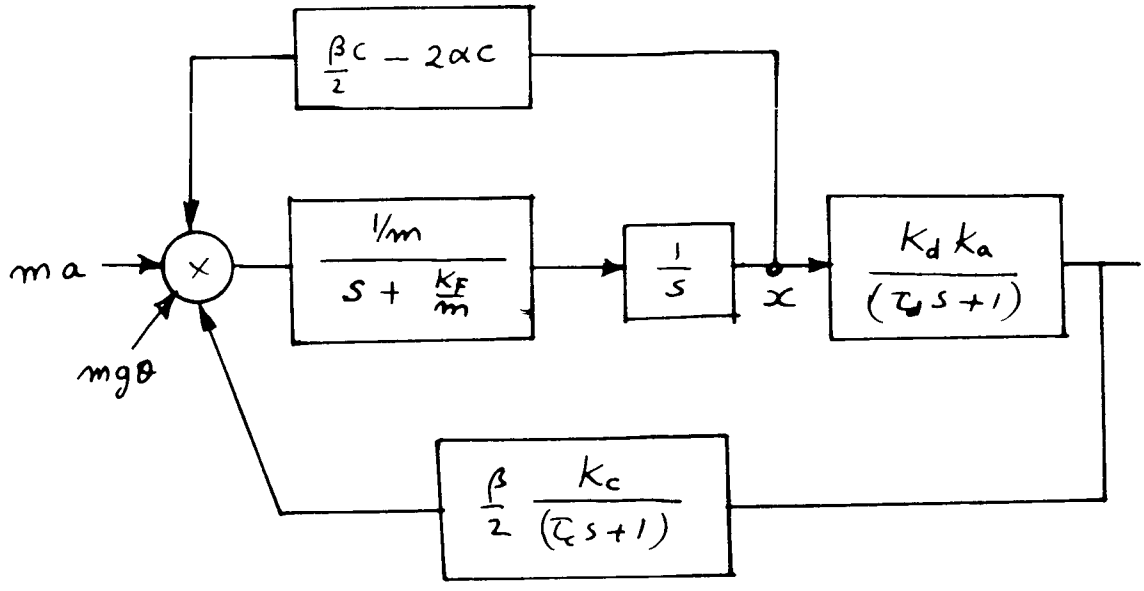

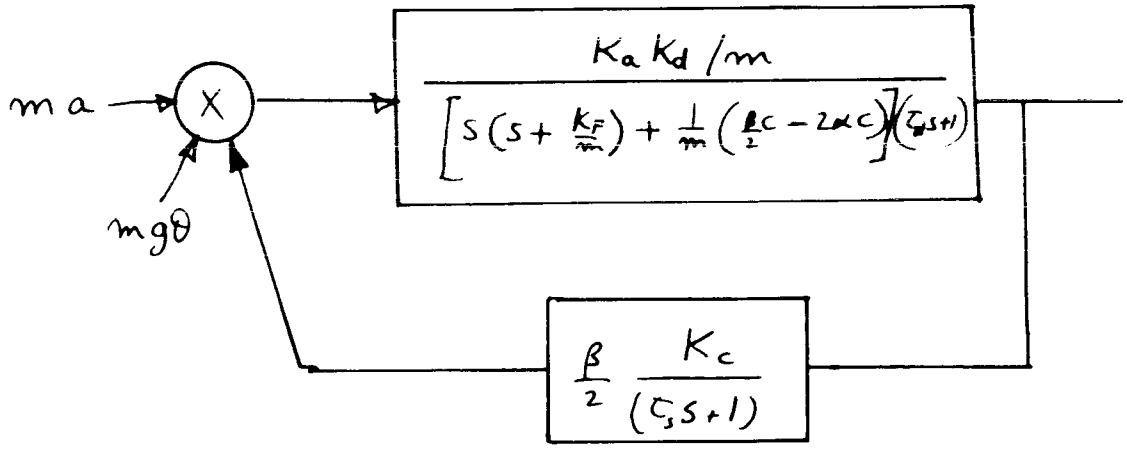

FIG 6.2-2 SIMPLIFIED LINEARIZED MODEL

is incorporated, the root locus diagram in Figure 6.2-3b is modified by the lead network zero on the negative real axis to give a system that is stable for higher gain than previously, see Figure 6.2-4. The open loop transfer function becomes

$$\frac{\frac{\beta}{2} K_a K_d K_c \frac{1}{m} \left(\tau_L s + 1\right)}{\left[s^2 + \frac{k_F}{m} s + \frac{1}{m}\left(\frac{\beta}{2} c - 2\alpha c\right)\right]\left(\tau_d s + 1\right)\left(\tau_c s + 1\right)}$$

τ_L = lead compensation time constant

6.3 Steady State Displacement Error

The steady state displacement error for a step input is given by

$$x_{ss} = \lim_{s \to 0} s \left[\frac{\frac{1/m}{\left[s\left(s + \frac{k_F}{m}\right) + \frac{1}{m}\left(\frac{\beta}{2} c - 2\alpha c\right)\right]}}{1 + \frac{\frac{\beta}{2} K_a K_d K_c \frac{1}{m} \left(\tau_L s + 1\right)}{\left[s\left(s + \frac{k_F}{m}\right) + \frac{1}{m}\left(\frac{\beta}{2} c - 2\alpha c\right)\right]\left(\tau_d s + 1\right)\left(\tau_c s + 1\right)}}\right] \frac{ma}{s}$$

$$= \frac{a}{\frac{\beta}{2} K_a K_d K_c \frac{1}{m}}$$

so that x can be small for a high loop gain. If the steady state error is to be zero, a pole at the origin has to be added and this brings another stability problem.

6.4 Measurement of Acceleration

The differential current in the coils is a measure of the applied acceleration.

The output of the accelerometer is obtained by measuring this current or less accurately, by measuring the voltage output of the amplifier in the loop.

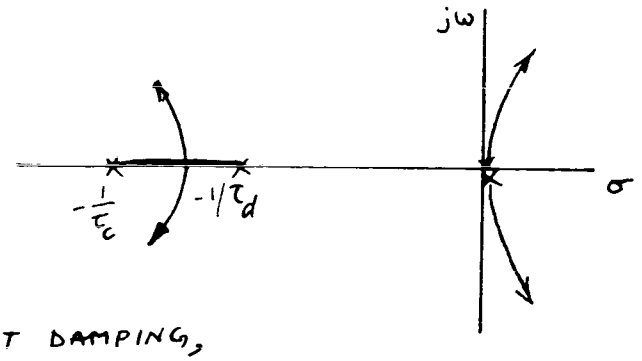

(a) WITHOUT DAMPING, SUSPENSION AND COMMON MODE FORCES

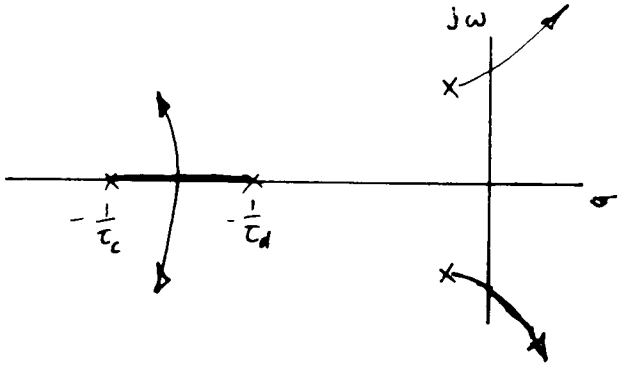

(b)

FIG 6.2— 3 ROOT LOCUS SKETCHES BEFORE COMPENSATION

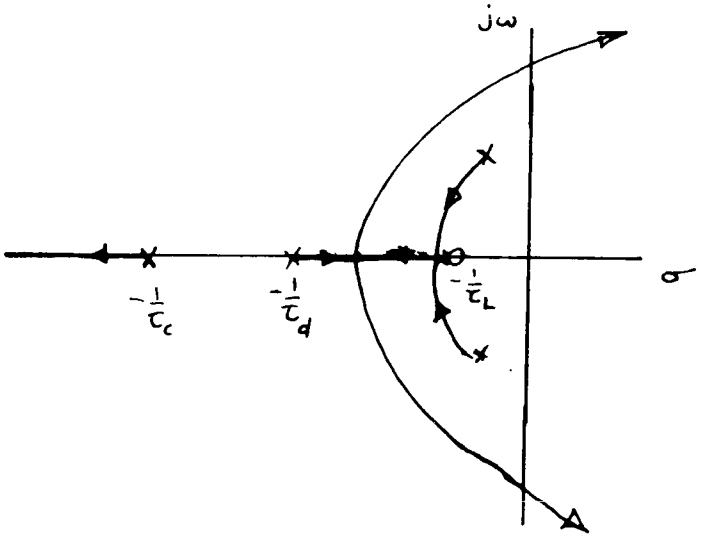

FIG 6·2 — 4 ROOT LOCUS SKETCH AFTER LEAD COMPENSATION

CHAPTER 7

PERFORMANCE OF THE ACCELEROMETER

7.1 Preliminary Experiments

Preliminary experiments were performed in a glass dewar[1] to determine the float height, the tube geometry, methods for magnet insertion and so on. Quantitative data became available when the metal dewar was operational.

7.2 Determination of the Effective Spring Constant

The effective spring constant was determined by measuring the natural frequency of oscillation of the magnet after it has been displaced by a finite distance. Because of the nonlinearity of the forces inside the tube, it was essential to keep the amplitude as small as possible. By using the displacement detector, an amplitude of 1 mm was ensured. For a true evaluation, an amplitude of less than 1 micron is desirable.

The positions of the coils were fixed so that the closer end of each coil was about 2 cm from the center of the tube. The currents in the coils were made equal and the dewar was tilted until the magnet, in its rest

position, aligned itself with the center of the linear range of the detector.

The magnet was then withdrawn to one end of the displacement detector range by means of another magnet outside the dewar. This external magnet was then removed and the resulting oscillation of the magnet inside the dewar was recorded, see Figure 7.2-1.

This procedure was repeated for various values of common mode current. The magnet became unstable when the current dropped below 11 mA, that is when the magnitude of the coil force approached that of the negative suspension force.

Figure 7.2-2 shows a plot of the effective spring constant K, [mass of magnet x (natural frequency)^2] against the common mode current. The curve closely approximates a straight line, thus indicating that the net force on the magnet is linear inside a 1 mm region around null. The curve also shows that for a current of 10 mA the spring constant would be zero. The intercept on the K axis gives the negative suspension spring constant, -15 dynes/cm. at that displacement.

The lowest value of spring constant obtained before the magnet became unstable was 2 dynes/cm. The general vibration of the surroundings probably dictated the lowest value of spring constant that could be measured.

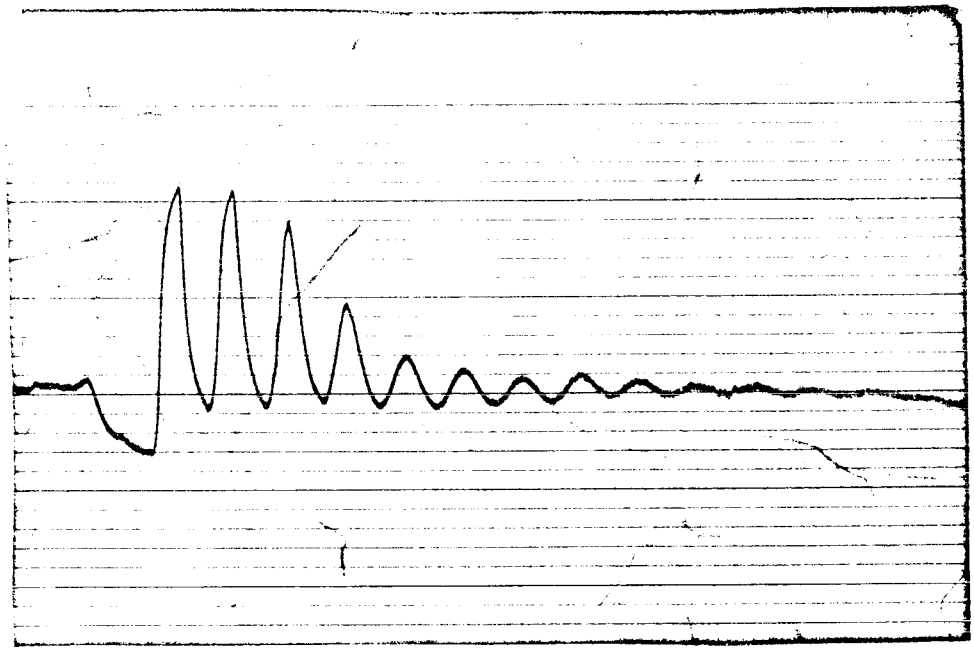

Figure 7.2-1 Open Loop Oscillation for a Given Common Current

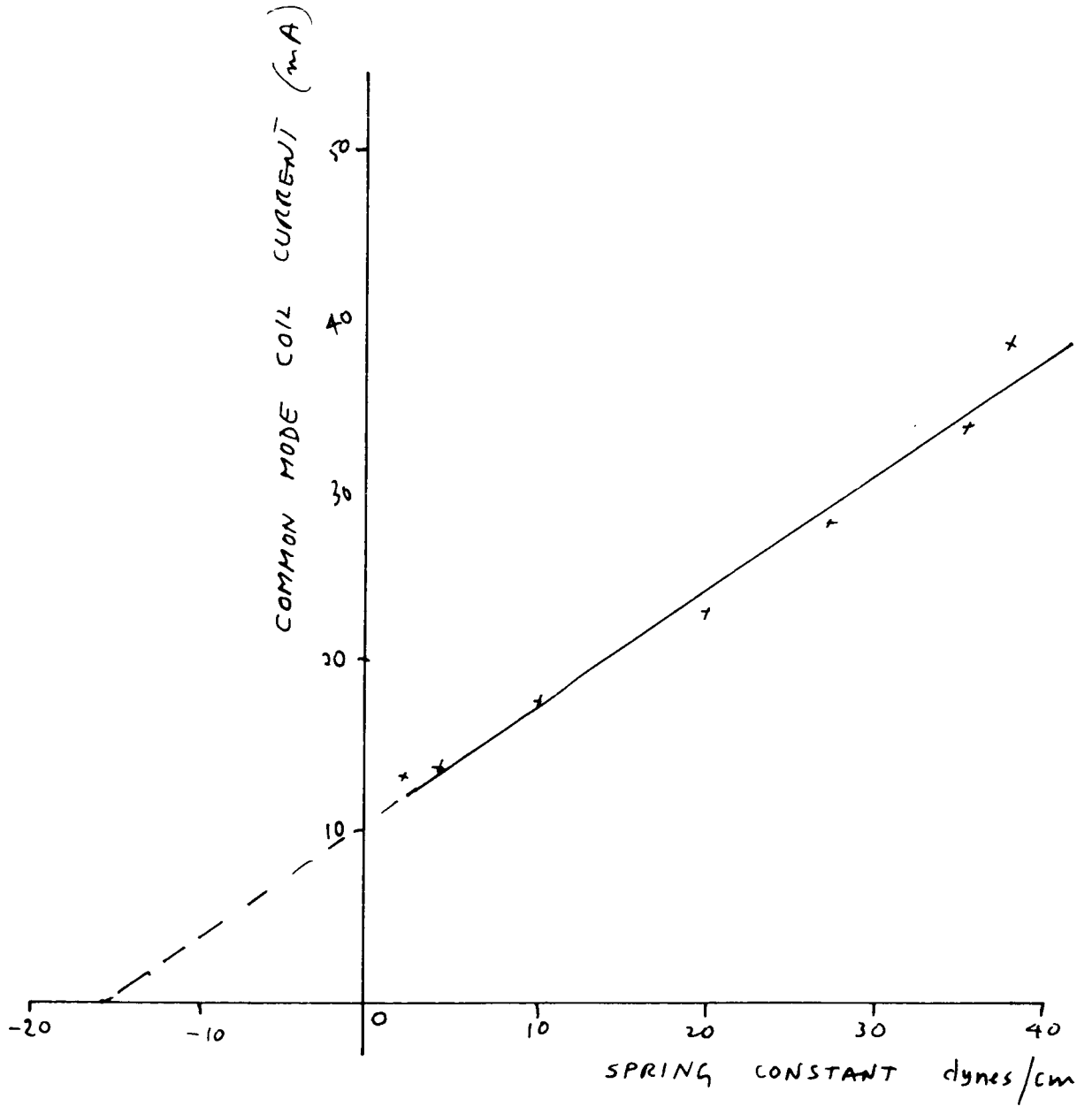

FIG 7.2-2 SPRING CONSTANT AGAINST COMMON MODE COIL CURRENT

7.3 Determination of the Damping Constant

Eddy current damping information can be obtained from the recorded oscillations such as that in Figure 7.2-1. By measuring successive amplitudes of the damped oscillation and plotting $\log_e$ (amplitude) against time for different values of common mode current as shown in Figure 7.3-1. The damping time constant is found to be 3 seconds.

7.4 Open Loop Response to Applied Acceleration

With the setup as in Section 7.2 and with the common mode current around its lowest value for stability, various known tilt angles were applied. It was observed that 12 seconds of arc gave a detectable change in the output of the displacement detector. This angle of tilt corresponds to 6×10^{-5} g.

7.5 Closing the Loop

In order to close the loop around the magnet, the output of the displacement detector was fed into a variable gain operational amplifier, see Figure 7.5-1. The amplifier output drove a differential transistor stage. The two coils were connected in series across the two collectors of the transistors and the point between the coils was connected to a variable voltage supply.

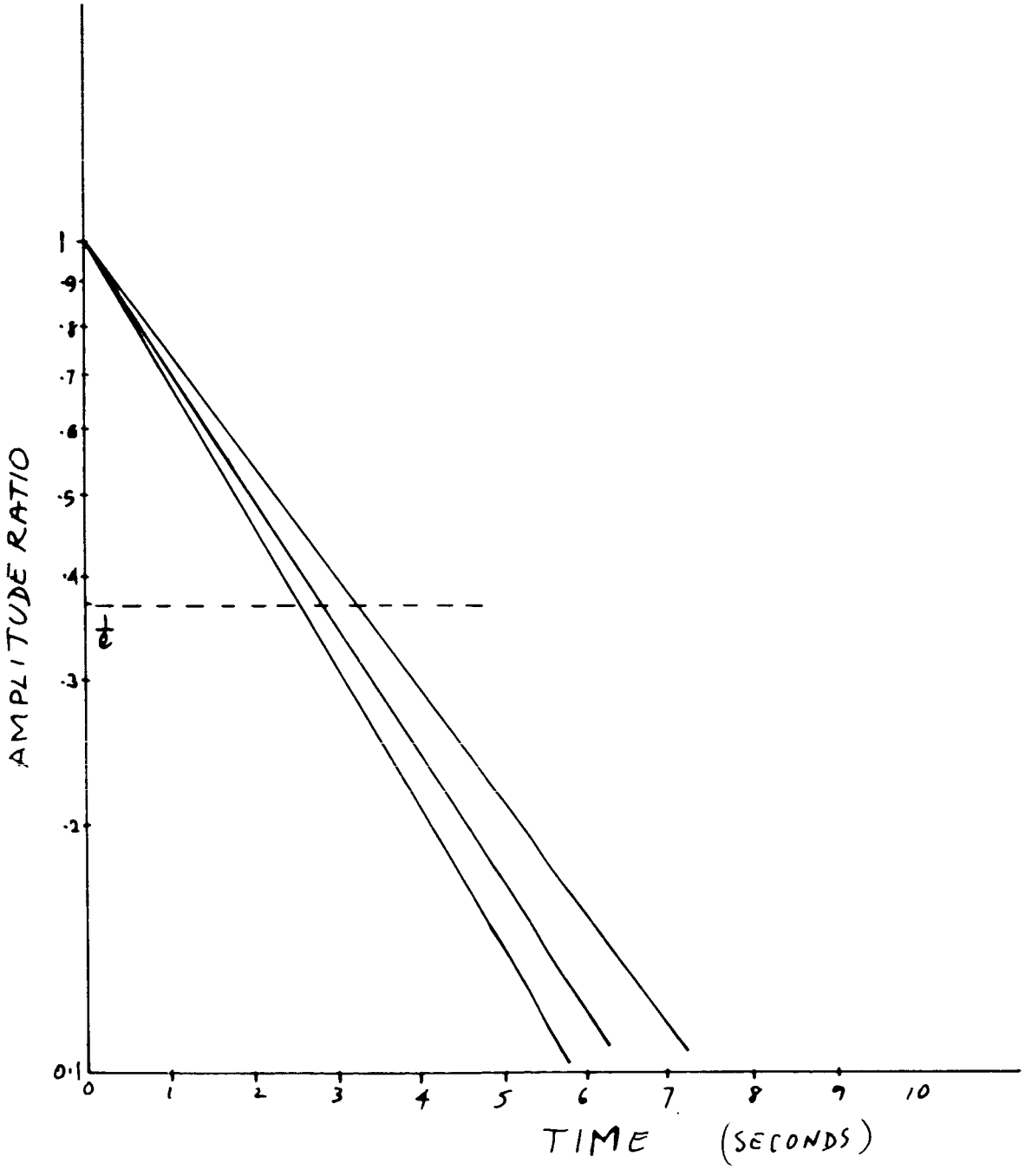

FIG 7.3 – 1 AMPLITUDE RATIO AGAINST TIME

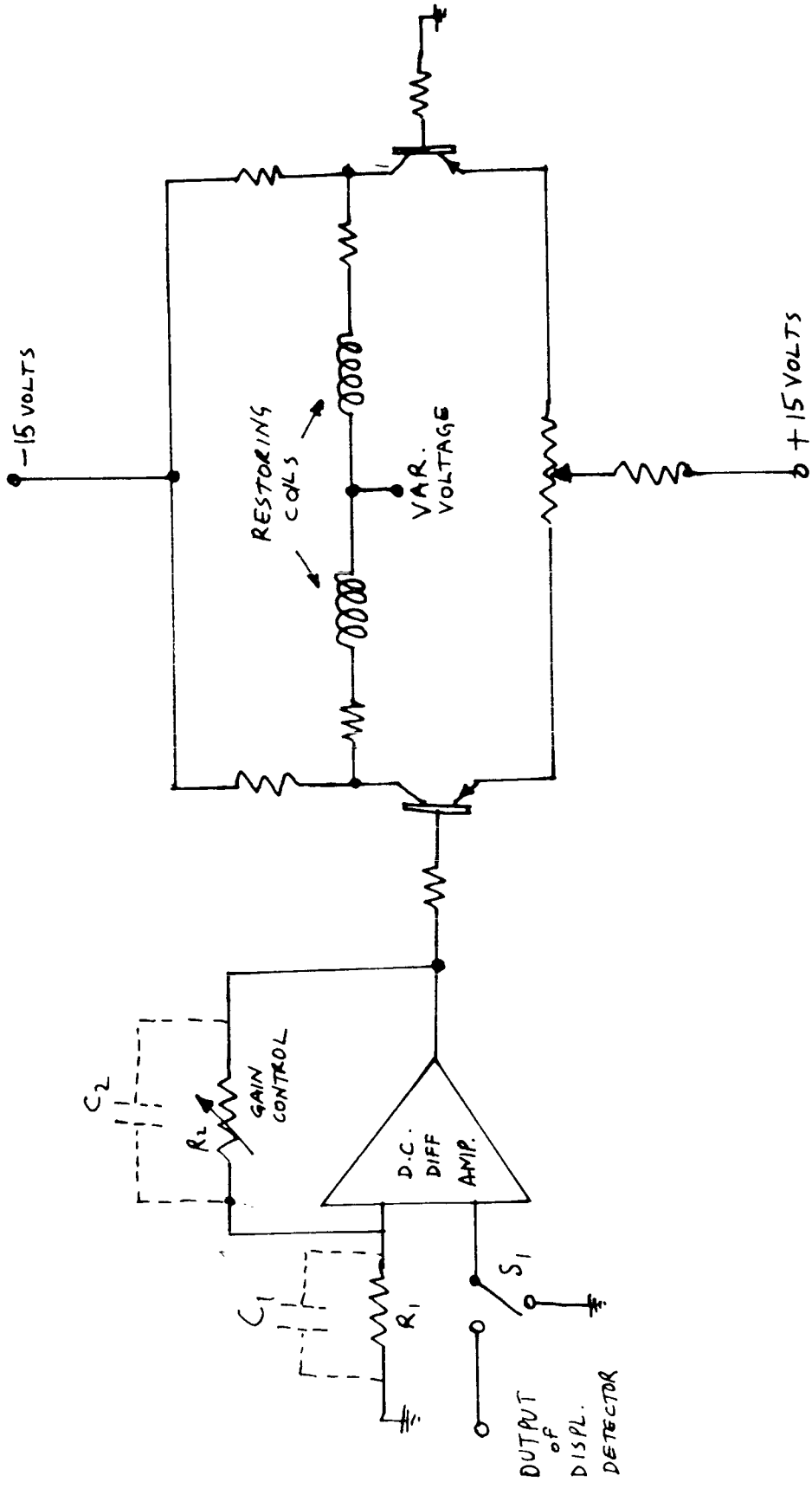

FIG 7.5-1 FEED BACK LOOP ELECTRONICS

In the open loop mode, the input to the amplifier was grounded by closing switch S_1 and the input to the differential stage was also zero. The common mode current in the two coils was adjusted by means of the applied voltage at the centre point between the coils.

In the closed loop mode, switch S_1 was opened so that a displacement detector output would cause a differential current in the coils.

Starting with the same procedure as for Section 7.2, the magnet was brought into the linear range of the detector and the loop was closed.

The output of the displacement detector was monitored on a recorder. The output clearly indicated the presence of a limit cycle shown in Figure 7.5-2 due to the limiting property of the detector. Turning the gain down only reduced the frequency of the oscillation.

By applying a lead, capacitor C_1 across R_1, and adjusting the gain, the oscillation began to damp out, see Figure 7.5-3, as was predicted in Chapter 6. However, before the loop was stabilized completely, the magnet was excited into another mode of oscillation -- about a horizontal axis normal to the tube, as shown by the sudden appearance of a high frequency oscillation, which will be investigated in the following section. This mode of oscillation was eliminated by the application of a low pass filter in the feedback loop, C_2 across R_2, and the

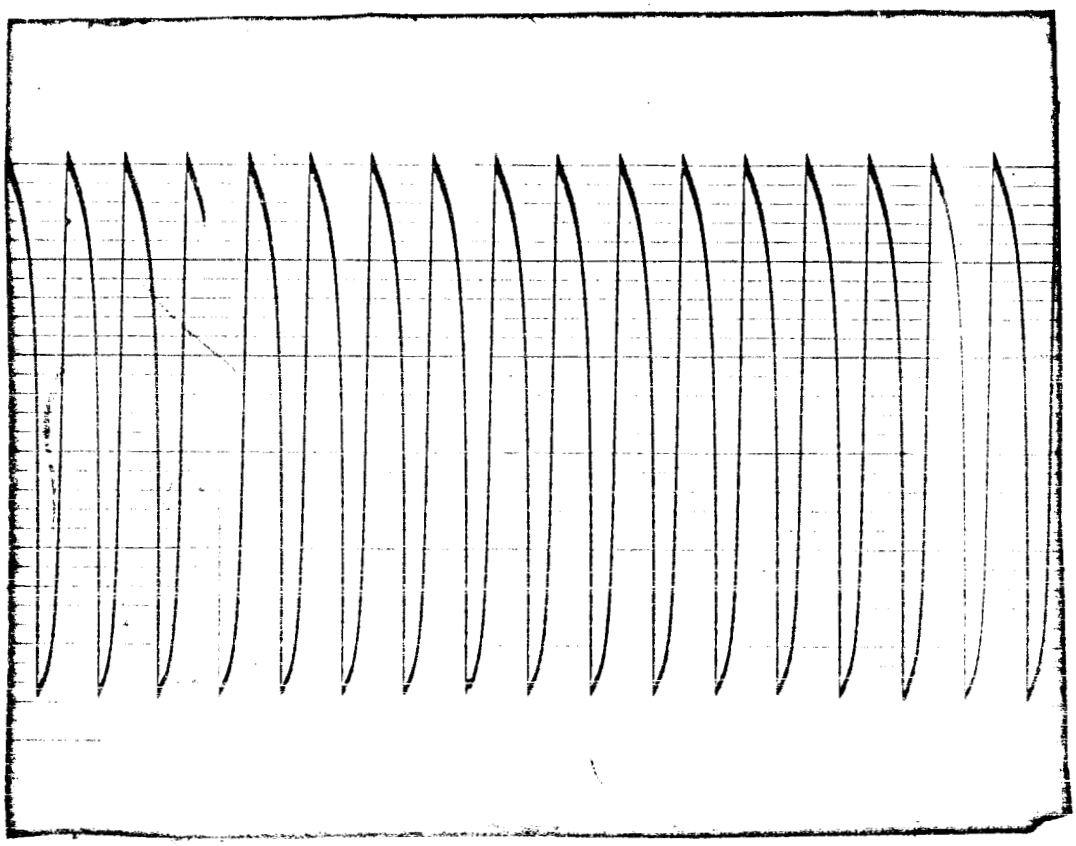

Figure 7.5-2 Closed Loop Limit Cycle

loop was finally stabilized. The magnet was quite stationary, with the usual slight oscillation about the sensitive axis since damping is not provided for this mode in the present suspension.

The application of tilt angles of about 50 seconds of arc gave noticeable change in the detector output but an accurate closed loop response to step acceleration inputs has yet to be determined.

The variation in the frequency of the damped oscillation in Figure 7.5-3 may be explained as follows: for small amplitudes, well within the linear range of the displacement detector, the frequency was about 2.5 c/s due to a fairly tight loop with an effective spring constant of 250 dynes/cm. As the amplitude increased, the curvature of the detector output, Figure 5.4.2-3, had the effect of decreasing the net gain in the loop thus decreasing the spring constant and hence the natural frequency.

7.6 Analysis of the Excited Mode of Oscillation

The excited mode of oscillation was most probably caused by the detector being sensitive to rotations and displacements about other axes. Assuming the magnet is stabilized at null with the loop closed and allowing a

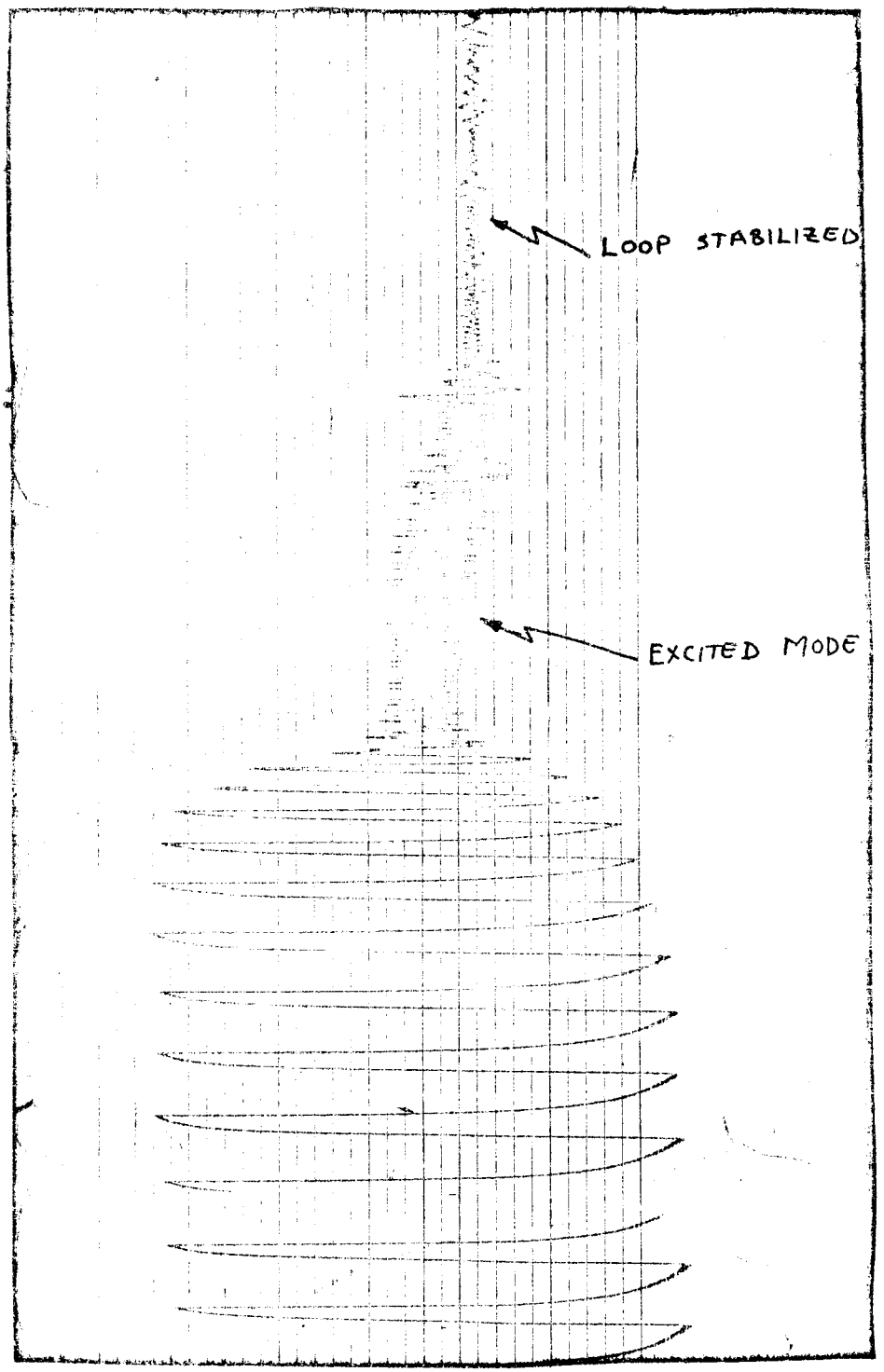

Figure 7.5-3 Damping of Closed Loop Oscillation

slight rotation of the magnet about the transverse horizontal axis, Figure 7.6-1, the detector output is reduced and a differential current force is exerted on the magnet tending to push it back to null. With the magnet in this position, the stabilizing force will now cause a torque tending to rotate the magnet even further. This rotation is checked by the tight radial suspension and the magnet is returned towards its normal position. As it goes past null, the same behavior takes place for rotation in the opposite direction. The effect soon builds up until resonance is achieved. Coupled with the rotational oscillations there is also translational oscillations due to the other effect of the stabilizing force.

The resonant frequency was 7 c/s so that the radial spring constant was 2000 dynes/cm indicating a tight radial suspension.

This mode of oscillation was eliminated by filtering since in doing so the phase of the torque was altered and the condition for sustaining the oscillation disappeared.

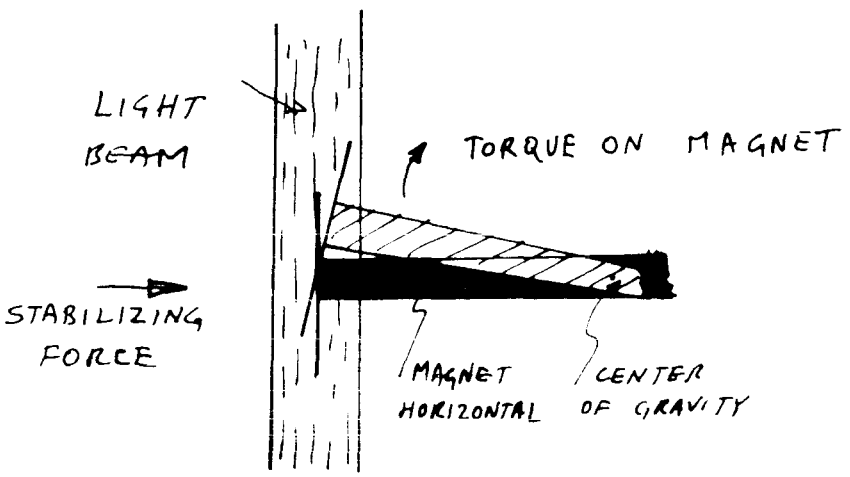

ROTATION OF MAGNET CAUSES A REDUCTION IN DETECTOR OUTPUT

FIG 7.6-1 SENSITIVITY OF DETECTOR TO ROTATION OF MAGNET

CHAPTER 8

CALIBRATION

8.1 General

As was mentioned earlier, the force generated by the restoring coils cannot be accurately determined. The steady state differential current in the coils, when in closed loop operation, is a measure of the applied acceleration. For the purpose of calibration, an external force of known magnitude is exerted on the magnet and the corresponding differential current recorded. This can be repeated for other magnitudes of the force to obtain a calibration curve.

Since the mass of the magnet is 1 gram, an external force of 10^{-3} dynes corresponds to an acceleration of 10^{-6}g.

Considering the methods of generating small forces outlined in Chapter 3, and keeping in mind that the range of interest extends below 10^{-6}g, the photon force provides a feasible solution.

Possible methods for generating a suitable photon force for LLAMA application are examined in the following sections.

8.2 Requirements for Application of Photon Force

Several requirements have to be met for the application of photon force.

(a) The available surface area dictates the power density in the beam. In LLAMA, because of float height limitation in the present setup, the available surface is a disc 1 cm in diameter or an area of 0.78 cm^2. The area of the largest square inscribed in the disc is 0.51 cm^2. To generate low forces is simple. To generate 10^{-3} dynes requires 1.5 watts, see Section 3.3.1 for a perfectly reflecting surface and the power density is 2-3 watts/cm^2 depending on the cross-section of the beam. Possible sources are discussed in Section 8.3.

(b) A high vacuum environment below 10^{-5} torr must prevail, to avoid thermal effects, see Section 2.3.3. The vacuum surrounding the liquid helium inner bottle is excellent since after a short period of time only helium gas can exist in this region, since all other gases liquify due to the cryopumping action of the liquid helium. To ensure the absence of helium gas, the enclosure can be flushed with, say nitrogen.

However, in the present system, air which is rich in helium due to the evaporation of liquid helium from the inner bottle, can leak in from outside via the 'o' ring feed throughs and a helium atmosphere can build up. If found necessary, a low pressure pump can be permanently incorporated so as to keep the vacuum as low as desired.

(c) The surface must have a high work function so as to reduce the generation of photo-electrons, see Section 3.3.2.

8.3 Criterion for Choice of Source

A good source of photons is a light source. Source of light vary in brightness, size of source, spectral distribution of the radiated energy, the direction of the radiation and so on.

In the case of LLAMA, the photon beam not only has to be squeezed on to an area less than 1 cm^2, but also has to meet a beam angle requirement imposed by the geometry of the suspension.

In order to develop a criterion by which various sources may be judged, a simple optical configuration is assumed, see Figure 8.3.-1 where

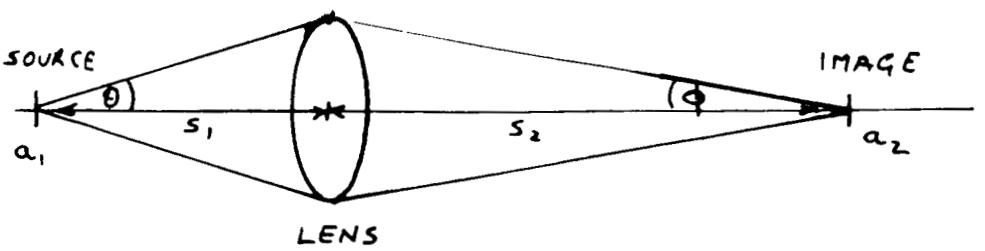

Figure 8.3-1 Optical Configuration for Comparison of Sources

a_1 = projected area of source normal to optical axis

B_1 = brightness of source

a_2 = projected area of image normal to optical axis

θ = angular semi-aperture of lens from source

= angular semi-aperture of lens from image

s_1 = distance of source from lens

s_2 = distance of image from lens

F = flux collected by lens

Assuming the source emits equally in all directions, i.e., a Lambert's Law radiator, the flux collected by an elemental ring at the lens is given by

$$\delta F = B_1 a_1 \cos\psi \, \delta\omega$$

where

ψ = angle subtended by ring

$\delta\omega$ = solid angle subtended by ring

r = distance of any element of ring from source

and

$$\delta\omega = \frac{2\pi r \sin\psi \; r \, \delta\psi}{r^2}$$

$$= 2\pi \sin\psi \, d\psi$$

The total flux collected by the lens is

$$F = 2\pi B_1 a_1 \int_0^{\theta} \sin\psi \cos\psi \, d\psi$$

$$= \pi B_1 a_1 \sin^2\theta$$

Now substituting for sin θ and noting that $\frac{a_2}{a_1} = \frac{s_2^2}{s_1^2}$

$$F = \pi B_1 a_1 \frac{\tan^2\phi}{\frac{a_1}{a_2} + \tan^2\phi} \qquad (8.3\text{-}1)$$

The flux collected by the image is FT where T is the transmission factor of the lens, provided the image is smaller or equal to the available image area.

For a given ϕ , equation 8.3-1 shows that F is increased if the product $B_1 a_1$ is maximized and

$\frac{a_1}{a_2} = \frac{1}{(\text{magnification})^2}$ is minimized.

For a given lens, there is a definite limit on the magnification for each value of ϕ. Figure 8.3-2 shows the magnification for different values of ϕ for an f/1 lens. Another limit on the magnification is the size of the target area.

Using Equation 8.3-1, the limitation on magnification from Figure 8.3-2, and assuming a target area of 0.25 cm^2, three promising sources were compared. All three were high pressure mercury arc lamps and their characteristics are given in Table 8.3-1

SOURCE	POWER WATTS	SOURCE DIMENSIONS mm	BRIGHTNESS cdls /cm²
I	100	0.25 × 0.25	170,000
II	200	0.6 × 2.2	33,000
III	500	1.1 × 4.1	30,000

Table 8.3-1

Figure 8.3-3 shows a plot of the flux collected by an f/1 lens (in arbitrary units) against ϕ for the three sources.

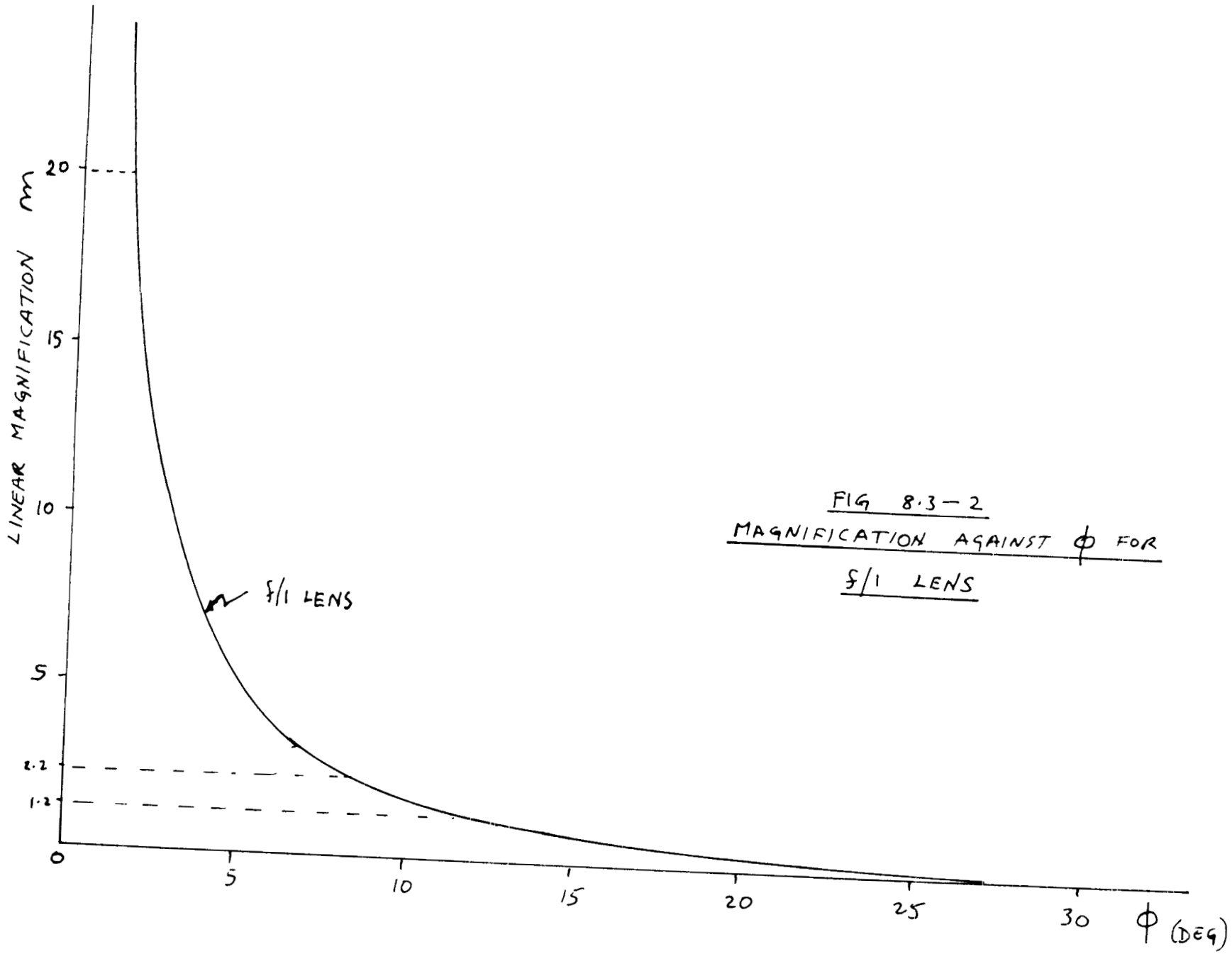

FIG 8.3-2
MAGNIFICATION AGAINST φ FOR
f/1 LENS

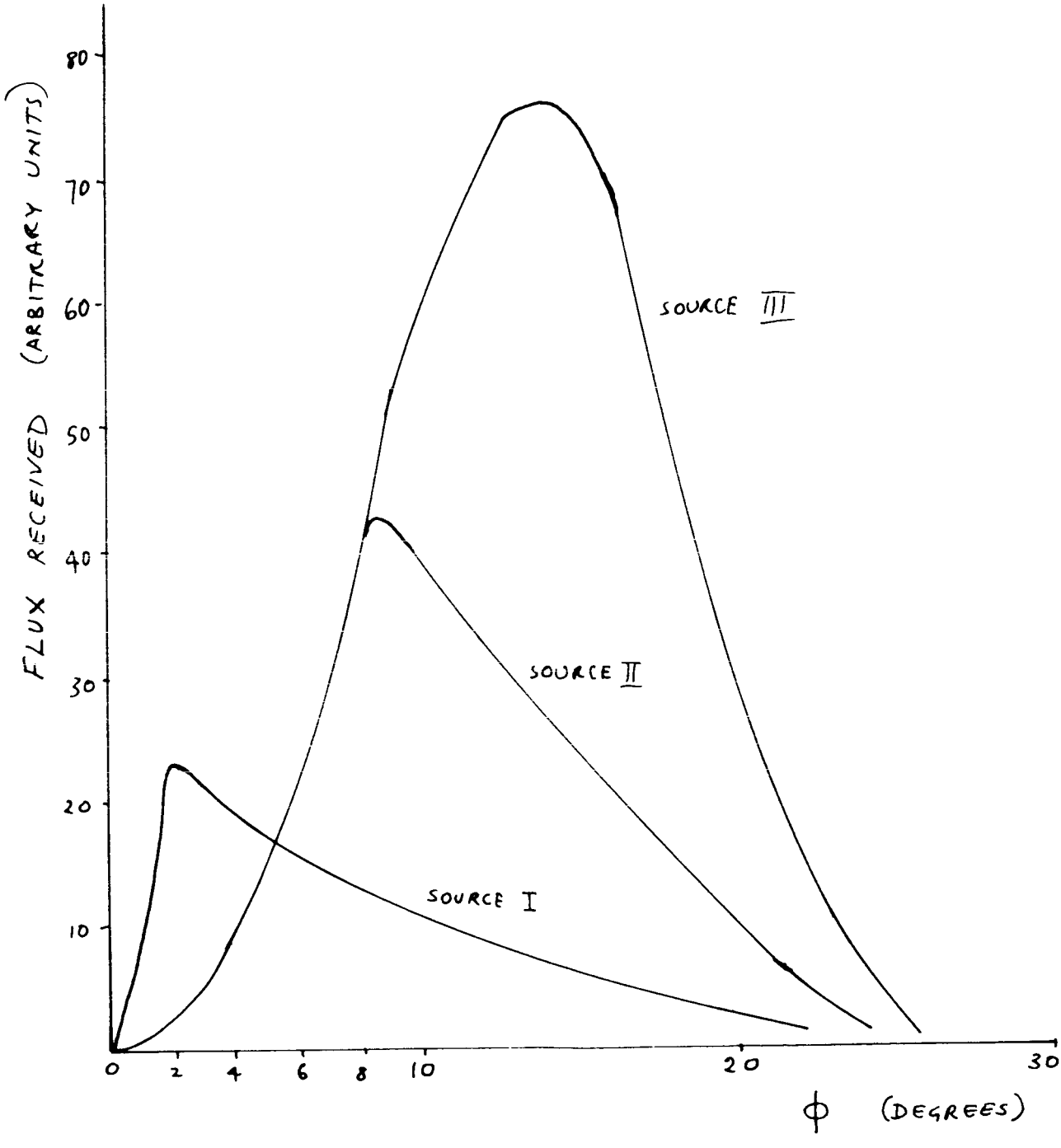

FIG. 8.3–3 FLUX RECEIVED AGAINST ϕ

With a 5 cm diameter, f/1 lens, the LLAMA geometry dictate a ϕ less than 6^{o}. Figure 8.3-3 shows that the 100 watt lamp collects the most flux in the region where ϕ is below 6 degrees.

8.4 Force Available from 100 Watt Arc Lamp

The optical configuration for the measurement of the power from the 100 watt arc lamp is shown in Figure 8.4-1 and a photograph of the setup is shown in Figure 8.4-2. The lamp was an Osram HBO-109 mercury arc lamp.

The radiation from the lamp was collected by an f/1 lens and focussed on a thermopile 20 cm away after attenuation by a neutral density filter. The back radiation was made use of by placing a spherical reflector with the source at its center of curvature. The image size was less than 0.25 cm^2 and the measured power was 3.5 watts. (This takes into account the attenuation of the filter.)

The lens used was uncoated and made from ordinary lens glass. A coated quartz lens would have increased the power by reducing the reflection at the lens, and the ultra violet absorption by the lens. The line spectra of the lamp extended to below $2900A^{o}$.

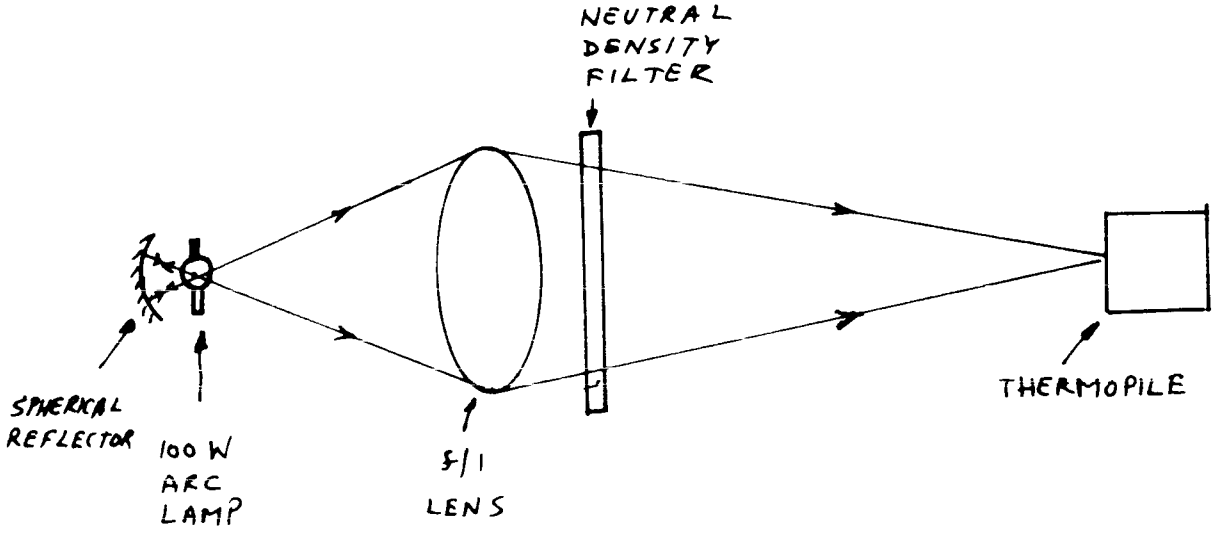

FIG 8·4–1 CONFIGURATION FOR MEASUREMENT OF POWER FROM 100 W LAMP

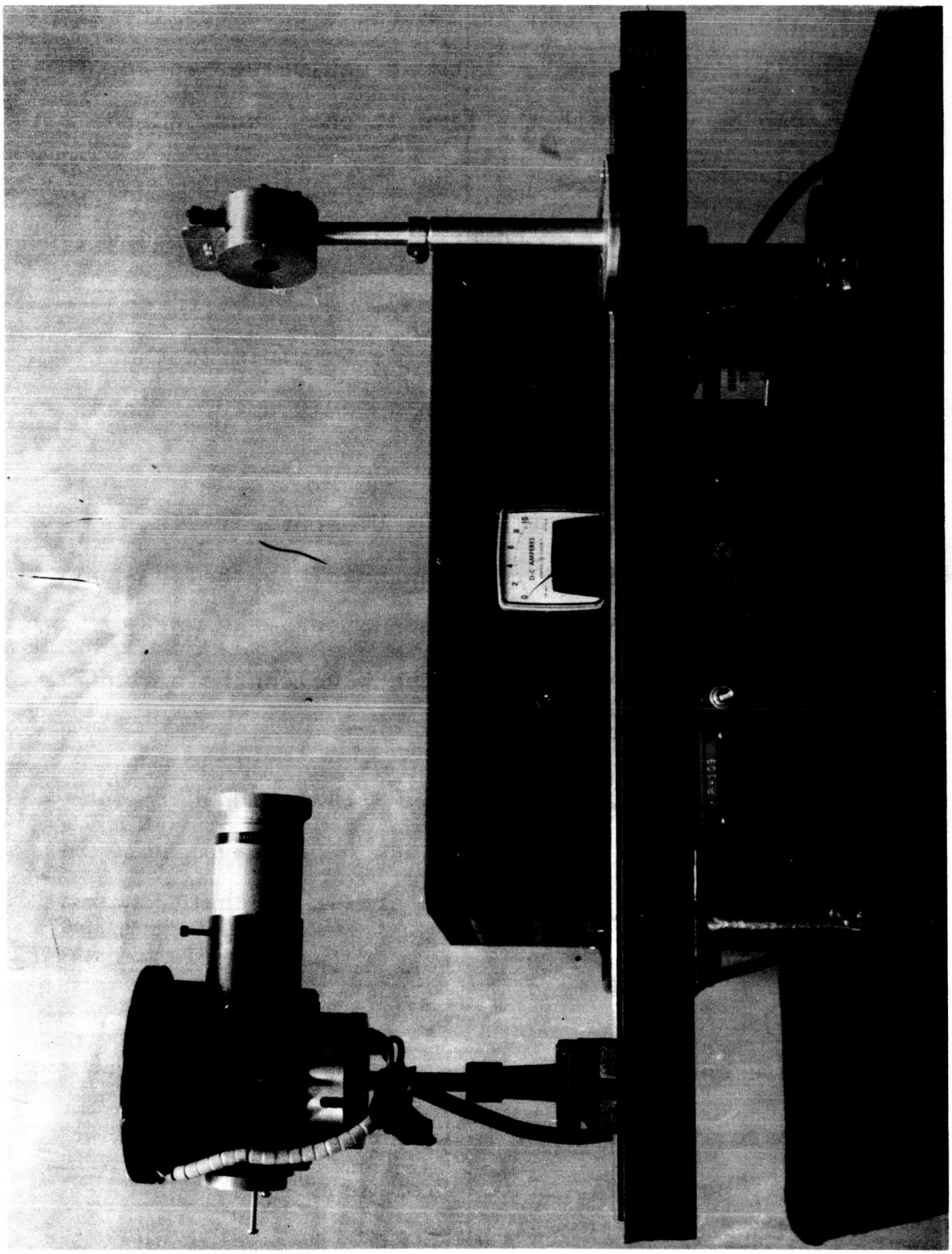

Figure 8.4-2 Setup for Measuring Power from Arc Lamp

To increase the power even more, a good quality aluminized elliptical reflector with an equivalent speed of f/ $\frac{1}{2}$ can be used with the lamp at one focus and the target at the other focus.

Already the measured power of 3.5 watts is equivalent to more than 2 x 10^{-3} dynes.

A UV source is preferred so as to minimize the heating effect inside the cryogenic environment to conserve the helium.

Another advantage for using a UV source is its compatability with the 8328A^{o} wavelength of the helium-neon laser that is proposed for use in the interferometer. The filtering problem is eased when the wavelengths of the sources are widely separated.

Other sources that can give a slightly higher power density in a beam angle of less than 6^{o} are available in the form of high intensity carbon arc lamps that consume around 14,000 watts.

8.5 Measurement of Photon Force

By measuring the power in a photon beam, the force it can exert can be calculated from Equation 3.3.1-1.

The ideal detector is one that has a flat response for all wavelengths in the beam, a high signal to noise

ratio and a short time constant.

Quantum detectors such as photo-electric, photo-conducting and photo-voltaic cells where the incident photons change the detector characteristic directly exhibit different sensitivities for different wavelengths. This property is undesirable unless the beam is monochromatic.

Thermal detectors, such as a thermopile, absorb the radiation in a black surface and detect the temperature rise in the surface by the Peltier Effect. A surface such as lamp black absorbs equally over a wide range. One disadvantage with thermal detectors is the inherent time constant of the order of a second which can become troublesome when the beam is modulated. The noise level is negligible since the signal is high.

8.6 Modulation of Photon Force

The search for a simple nonmechanical method for the control of the intensity of a photon beam is intense.

Electro optical techniques, however, do exist using the Kerr cell[11] or the Pockels effect where the light is first polarized by a 0° polarizer, passes through 0°-90° variable polarizer and finally through a 90° polarizer. By varying the angle of the polarization[12] in the middle polarizer, the intensity of the beam can be modulated. The maximum transmission is about 25%.

Mechanical shutters are numerous and can be used either as aperture controllers or as choppers. A suitable method for generating pulses of varying widths from a constant beam can be achieved using a stepping motor.[13]

Sources such as flash tubes can be easily controlled by varying the flash rate but the average power output for a period of time is below 1 watt with present devices.

The application of injection lasers is discussed in the next section.

8.7 Injection Laser Application

Injection lasers are ideal for the generation of photon force. The beam is narrow, intense and can be electronically modulated. The fact that the radiation is not highly monochromatic or coherent is of little consequence.

Present injection lasers have reached an output power of 3 watts[14] continuous -- but these devices are still in the experimental stage.

The cryogenic cooling that is required for the lasers presents no problem in this case since liquid helium and nitrogen are already available for the suspension.

8.8 Possible Calibration Method

To generate a low level force of 10^{-3} dynes and less of known magnitude is one problem, to use this force for calibration on earth is another problem.

Assuming ideal conditions where the outside interference is negligible during time needed for calibration, a possible method is shown in Figure 8.8-1.

The photon beam is directed at an aluminum deposited disc attached at one end of the magnet. A well-calibrated beam splitter deflects 1% of the beam onto a thermopile. This deflected beam is made to pass through identical windows, rejection filters, and so on as those in the main beam for compensation. The intensity of the beam can be varied by neutral density filters and the differential current required to keep the magnet at null is recorded so as to obtain a calibration curve. If the differential current is too small, the number of turns in the coils can be reduced.

If the isolation is not ideal, an alternating force can be applied by chopping the photon beam. The frequency has to be chosen so that it can be easily filtered out. The choice of frequency depends on the statistical behavior of the interference for the particular environment selected and on the bandwidth of the accelerometer. A survey of various disturbances and a means for building an isolation platform is given in Ref. 15.

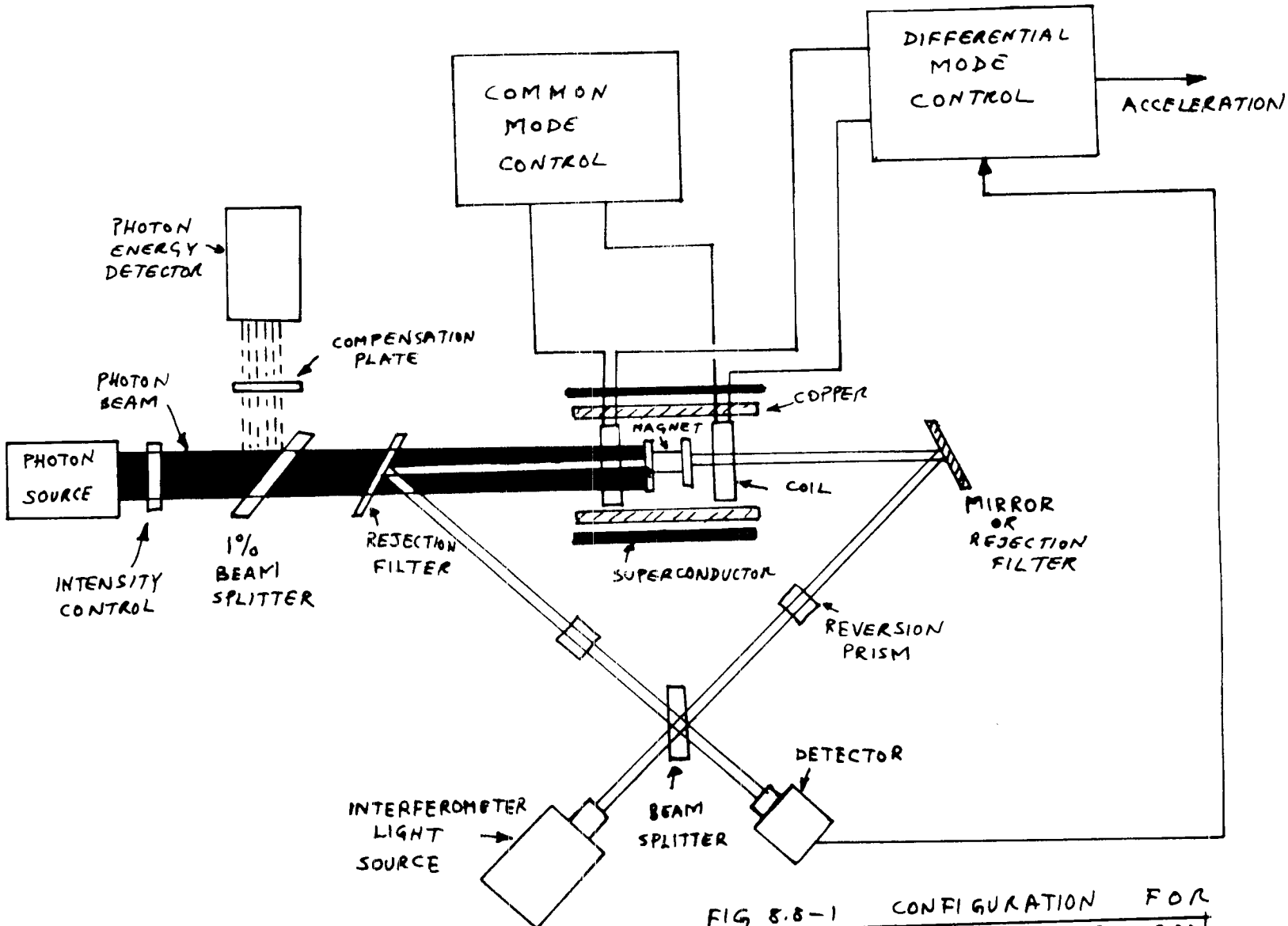

FIG 8.8-1 CONFIGURATION FOR LLAMA CALIBRATION

CHAPTER 9

CONCLUSIONS AND FURTHER WORK

The experiments that have been carried out so far were of a preliminary nature. The precise location of null, accurate levelling of the superconducting tube and accurate positioning of the restoring coils are needed before data can be reliably interpreted. However, unless a stable vibration isolated base is used, there is not much to be gained from such fine adjustments. The availability of a more sensitive displacement detector would enable the close examination of the region around null, for in this region lie the advantages and the ultimate limitations of the accelerometer.

With the crude form of the accelerometer that was used, an open loop threshold sensitivity of 10^{-5}g was observed.

The successful closing of the loop around the magnet showed that it was feasible to stabilize a test mass with 3 degrees of freedom along one axis. The mode of oscillation about the transverse horizontal axis that was excited was due to the detector being sensitive to rotation of the

magnet about that axis. This oscillation was eliminated by delaying the phase of the restoring force.

A closed loop step input response and a frequency response for different values of lead compensation would contribute to better understanding of the dynamics of the accelerometer.

The use of photons for generating a measureable low level force for calibration was investigated. Experiments with a 100 watt arc lamp demonstrated that sufficient power density was available from the lamp for calibration up to 10^{-6}g.

APPENDIX A

CORPUSCULAR CONCEPT OF LIGHT PRESSURE

The corpuscular concept[16] of light (or electromagnetic radiation) assumes that light consists of particles referred to as photons or light quanta. The evidence for this theory is in the photo-electric effect, the Compton effect, scintillation effect, etc.

The energy, E, of a photon is found to be proportional only to its frequency ν so that

$$E = h\nu \tag{A-1}$$

where h is Planck's constant.

The velocity of a photon v is that of the velocity of light c and therefore the mass m of a photon is given by the relativistic equation

$$m = \frac{m_o}{\sqrt{1 - \frac{v^2}{c^2}}} \tag{A-2}$$

where m_o is the rest mass of the photon and $v \longrightarrow c$.

The momentum of a photon ξ is given by

$$\xi = mv = \frac{m_o}{\sqrt{1-\frac{v^2}{c^2}}}\, v \qquad \text{(A-3)}$$

The total energy of a photon is given by the Einstein equation

$$E = mc^2 = \frac{m_o}{\sqrt{1-\frac{v^2}{c^2}}}\, c^2 \qquad \text{(A-4)}$$

Eliminating m_o from (A-3) and (A-4) gives

$$\xi = \frac{Ev}{c^2} \longrightarrow \frac{E}{c} \qquad (v \to c) \qquad \text{(A-5)}$$

(This is only valid if $\frac{m_o}{\sqrt{1-\frac{v^2}{c^2}}} \neq \infty$ when v = c so that as $v \longrightarrow c$, $m_o \longrightarrow o$, hence the assumption that a photon has zero mass). Equations (A-1) and (A-5) give

$$\xi = \frac{E}{c} = \frac{h\nu}{c} \qquad \text{(A-6)}$$

If now a photon impinges normally on a perfectly <u>absorbing</u> surface, the pressure exerted by the photon on the surface is the change in momentum in that direction. Therefore the pressure p is given by

$$p = \frac{E}{c}$$

If the surface has refelctivity r the pressure becomes

$$P = \frac{E}{c}(1+r)$$

or

$$P = \frac{h\nu}{c}(1+r)$$

If now, a beam of photons of density ρ and cross-section area A impinges normally on this surface, the total number of photons impinging on the surface is ρ c A. Therefore the pressure P exerted on the surface per unit area is given by

$$P = c\rho\frac{h\nu}{c}(1+r)$$
$$= \rho h\nu(1+r)$$

The energy in the beam per unit area is W where

$$W = \rho c h\nu$$
$$\therefore \quad P = \frac{W}{c}(1+r)$$

If W is in watts/cm^2, c in cm/sec, P is in dynes/cm^2 or given by $P = \frac{W}{c}(1+r)\times 10^7$

Example If W = 1 watt/cm^2, c = 3 x 10^{10}cm, r = 1

$$\therefore \quad P = \frac{2}{3}\ 10^{-3}\ \text{dynes}$$

REFERENCES

1. Chapman, P.K., A Cryogenic Test Mass Suspension for a Sensitive Accelerometer, S.M. Thesis June 1964, Dept. of Aeronautics and Astronautics, M.I.T.

2. Shoenberg, D., Superconductivity, Cambridge University Press, 1962.

3. Bremer, J.W., Superconductive Devices, McGraw-Hill, 1962.

4. Frisch, D., Notes on Film Radiation Pressure, M.I.T. Science Teaching Center, 1958.

5. Tear, J.D., A Torsion Balance for Measuring Radiation Pressure, JOSA August 1925.

6. Pearson, E., S.B. Thesis, Mechanical Engineering, M.I.T. 1958.

7. King, J.G. and Zacharias, J.R., Advances in Electronics and Electron Physics, Vol. VIII, Academic Press, 1956.

8. Blitch, M.G. and Keyes, W.R., Accelerometer Testing for Low-Level Inputs, Symposium on Inertial Components, M.I.T., May 1964.

9. Cunningham, W.J., Introduction to Nonlinear Analysis, McGraw-Hill 1958.

10. Mitchell, A., M.I.T. Department of Aeronautics and Astronautics, Special Projects, June 1964.

11. Electro-Optic Light Modulators, Bulletin 1201, ISOMET Corp. Palisades Park, New Jersey.

12. Shurcliff, W.A., Polarized Light, Harvard University Press, 1962.

13. Cyclonome Stepping Motor, Sigma Instruments, Braintree, Massachusetts.

14. Hall, R.N., Private Communication, December 1963.

15. Tsutsumi, K., A Ground Tilt Isolation Platform, M.I.T. Instrumentation Lab. Report E-1508, January 1964.

16 Harnwell and Livingwood, Experimental Atomic Physics, McGraw Hill, December 1961.